Research Report

FHWA Contract DTFH61-03-C-00104
Research Task No. 7
Retrofit of Rectangular Bridge Columns

RETROFIT OF RECTANGULAR BRIDGE COLUMNS USING CFRP WRAPPING

by

Mesay A. Endeshaw, Mohamed ElGawady, Ronald L. Sack and David I. McLean
Washington State Transportation Center (TRAC)
Washington State University
Department of Civil & Environmental Engineering
Pullman, WA 99164-2910

Prepared for
The Federal Highway Administration
U.S. Department of Transportation

Hamid Ghasemi, Project Technical Manager

December 2008

1. REPORT NO.	2. GOVERNMENT ACCESSION NO.	3. RECIPIENTS CATALOG NO
WA-RD 716.1		

4. TITLE AND SUBTITLE	5. REPORT DATE
Retrofit of Rectangular Bridge Columns Using CFRP Wrapping	December 2008
	6. PERFORMING ORGANIZATION CODE

7. AUTHOR(S)	8. PERFORMING ORGANIZATION REPORT NO.
Mesay A. Endeshaw, Mohamed ElGawady, Ronald L. Sack and David I. McLean	

9. PERFORMING ORGANIZATION NAME AND ADDRESS	10. WORK UNIT NO.
Washington State University Civil and Environmental Engineering PO Box 642910 Pullman, WA 99164-2910	11. CONTRACT OR GRANT NO. FHWA Contract DTFH61-03-C-00104, Task No. 7

12. CO-SPONSORING AGENCY NAME AND ADDRESS	13. TYPE OF REPORT AND PERIOD COVERED
Research Office Washington State Department of Transportation Transportation Building, MS 47372 Olympia, Washington 98504-7372 Project Manager: Kim Willoughby, 360-705-7978	Final Report
	14. SPONSORING AGENCY CODE

15. SUPPLEMENTARY NOTES

This study was conducted in cooperation with the U.S. Department of Transportation, Federal Highway Administration.

16. ABSTRACT

This study investigated retrofitting measures for improving the seismic performance of rectangular columns in existing bridges. Experimental tests were conducted on 0.4-scale column specimens which incorporated details that were selected to represent deficiencies present in older bridges in Washington State. Two unretrofitted specimens were tested to examine the performance of the as-built columns incorporating lap splices at the base of the columns and deficient transverse reinforcement. Five columns were retrofitted with carbon fiber reinforced polymer (CFRP) composite wrapping and one specimen was retrofitted with a steel jacket. The specimens were subjected to increasing levels of cycled lateral displacements under constant axial load. Specimen performance was evaluated based on failure mode, displacement ductility capacity and hysteretic behavior.

For retrofitting of rectangular columns, it is recommended that oval-shaped jackets be used whenever possible. Column specimens with oval-shaped jackets of steel and CFRP composite material performed similarly, both producing ductile column performance. Failure in these specimens was due to flexural hinging in the gap region between the footing and retrofit jacket, leading to eventual low-cycle fatigue fracture of the longitudinal reinforcement. Details and procedures for the design of oval-shaped steel jackets are provided in FHWA *Seismic Retrofitting Manual for Highway Bridges* (2006). Design guidelines for oval-shaped CFRP jackets are given in ACTT-95/08 (Seible et al., 1995). Oval-shaped jackets designed according to these recommendations can be expected to prevent slippage of lapped bars within the retrofitted region.

Design guidelines for rectangular-shaped retrofitting using CFRP composite materials are proposed for application to columns with cross-section aspect ratios of 2 or less. While no slippage of the lap splice was observed, it is conservatively recommended that rectangular-shaped CFRP wrapping be used only for the situation where controlled debonding of the lap splice is acceptable.

17. KEY WORDS	18. DISTRIBUTION STATEMENT
Carbon fiber reinforced polymer, bridge column retrofit	

19. SECURITY CLASSIF. (of this report)	20. SECURITY CLASSIF. (of this page)	21. NO. OF PAGES	22. PRICE
None	None		

DISCLAIMER

The contents of this report reflect the views of the authors, who are responsible for the facts and accuracy of the data presented herein. The contents do not necessarily reflect the official views or policies of the Federal Highway Administration. This report does not constitute a standard, specification, or regulation.

TABLE OF CONTENTS

LIST OF FIGURES

LIST OF TABLES

EXECUTIVE SUMMARY

This study investigated retrofitting measures for improving the seismic performance of rectangular columns in existing bridges. Experimental tests were conducted on 0.4-scale column specimens which incorporated details that were selected to represent deficiencies present in older bridges in Washington State. Two unretrofitted specimens were tested to examine the performance of the as-built columns incorporating lap splices at the base of the columns and deficient transverse reinforcement. Five columns were retrofitted with carbon fiber reinforced polymer (CFRP) composite wrapping and one specimen was retrofitted with a steel jacket. The specimens were subjected to increasing levels of cycled lateral displacements under constant axial load. Specimen performance was evaluated based on failure mode, displacement ductility capacity and hysteretic behavior.

Failure in the as-built specimens was caused by either spalling followed by longitudinal reinforcement buckling and eventual low cycle fatigue fracture or lap splice failure. Reasonable energy dissipation and ductility were achieved in the as-built specimens. While results from this study and from past research indicate satisfactory column performance for displacement ductility levels of 4 or more, these results should be applied carefully due to possible scaling effects, and it is anticipated that full-scale columns may perform worse than the scaled specimens. Hence, it is conservatively recommended that all columns be retrofitted to ensure a ductile performance for displacement ductility demands of 2 or more.

For retrofitting of rectangular columns, it is recommended that oval-shaped jackets be used whenever possible. Column specimens with oval-shaped jackets of steel and CFRP composite material performed similarly, both producing ductile column performance. Failure in these specimens was due to flexural hinging in the gap region between the footing and retrofit

jacket, leading to eventual low-cycle fatigue fracture of the longitudinal reinforcement. Details and procedures for the design of oval-shaped steel jackets are provided in FHWA *Seismic Retrofitting Manual for Highway Bridges* (2006). Design guidelines for oval-shaped CFRP jackets are given in ACTT-95/08 (Seible et al., 1995). Oval-shaped jackets designed according to these recommendations can be expected to prevent slippage of lapped bars within the retrofitted region.

Columns retrofitted with rectangular-shaped CFRP jackets all demonstrated ductile column performance. Failure in these specimens was due to flexural hinging in the gap region followed by low-cycle fatigue fracture of the reinforcement. The CFRP jacket designed based on ACTT-95/08 recommendations for rectangular-shaped retrofits resulted in satisfactory performance, but bulging of the CFRP jacket was observed towards the end of testing. Increased thickness of CFRP jackets resulted in reduced bulging of the CFRP jacket and, in the case of the specimen retrofitted with a CFRP jacket designed based on 150% of the ACTT-95/08 recommendations, improved performance.

Design guidelines for rectangular-shaped retrofitting using CFRP composite materials are proposed for application to columns with cross-section aspect ratios of 2 or less. While no slippage of the lap splice was observed, it is conservatively recommended that rectangular-shaped CFRP wrapping be used only for the situation where controlled debonding of the lap splice is acceptable.

INTRODUCTION

INTRODUCTION AND BACKGROUND

The 1971 San Fernando earthquake and other more recent earthquakes have demonstrated that bridges built according to older codes may be vulnerable to damage under seismic loading. Many of the interstate bridges in the United States were constructed in the 1950s and 1960s and incorporate deficiencies that must be addressed in order to avoid major damage or even collapse under a strong ground motion.

Common deficiencies found in bridge columns built prior to 1971 are insufficient transverse reinforcement and inadequate lap splice length. In addition, poor detailing including poor anchorage of the transverse reinforcement, rare use of ties, and lap splices located in potential flexural hinge regions make older columns susceptible to failure. Possible failure modes of deficient columns are shear failure, pre-mature flexural failure and lap splice failure.

It is not financially feasible to replace all deficient bridges, and hence retrofitting of existing deficient bridges is a necessary option. Several retrofitting techniques such as reinforced concrete jacketing and steel jacketing have been developed to rehabilitate structurally-deficient bridge columns. In the last decade or so, fiber reinforced polymers (FRP) have attracted the attention of researchers and bridge owners as an alternative material for retrofitting reinforced concrete bridge elements.

This report presents the findings of an experimental study conducted on rectangular bridge columns retrofitted using FRP composite materials. Eight 40% (1:2.5) scale slender columns representative of Washington State's interstate column inventory were tested. Two unretrofitted specimens were tested to examine the performance of the

as-built columns incorporating lap splices at the base of the columns and deficient transverse reinforcement. Five columns were retrofitted with carbon fiber reinforced polymer (CFRP) composite wrapping and one specimen was retrofitted with a steel jacket. All specimens were subjected to pseudo-static, reverse-cyclic loading. The performance of the tested specimens was evaluated based on failure mode, measured displacement ductility and hysteretic behavior.

RESEARCH OBJECTIVES

The overall goals of this study are to assess the seismic performance of existing slender rectangular bridge columns with known structural deficiencies and to evaluate the effectiveness of composite material retrofit measures for improving the performance of deficient columns. To achieve these goals, four objectives were established:

1) Identify the vulnerabilities of typical rectangular columns in bridges in Washington State built in the 1950s and 1960s under seismic loadings;
2) Evaluate CFRP composite wrapping as a retrofit measure for improving the seismic performance of rectangular columns incorporating lap splices at the base of the columns and deficient transverse reinforcement;
3) Compare the performance of columns retrofitted with CFRP composite wrapping to that for columns retrofitted with commonly used steel jacketing; and
4) Draw conclusions on the feasibility and effectiveness of CFRP composite wrapping for retrofitting deficient rectangular bridge columns.

REVIEW OF PREVIOUS RESEARCH

COLUMN DEFICIENCIES

Many older bridges were designed primarily for gravity loads with little or no consideration of lateral forces from seismic loading. As a result, older columns lack sufficient transverse reinforcement to provide satisfactory performance in a major seismic event. Typically, No. 3 or No. 4 hoops at 12 in. (0.3 m) on center were used in columns regardless of the column cross-sectional dimensions. The hoops were anchored by 90-degree hooks with short extensions which become ineffective once the cover concrete spalls. Furthermore, intermediate ties were rarely used. These details result in many older columns being susceptible to shear failure, and the hoops provide insufficient confinement to develop the full flexural capacity. The limited level of confinement is also unable to prevent buckling of the longitudinal reinforcement once spalling of the cover concrete occurs.

Another detail commonly used in the pre-1971 columns is splicing of the longitudinal bars at the base of the columns, which is a potential plastic hinge region. Starter bars often extended 20 to 35 times the column longitudinal bar diameter (d_b) from the footing. A lap splice length of $20d_b$ has been shown to be inadequate to transfer the full tensile force of the longitudinal reinforcement to the starter bars of the foundation (Haroun et al., 2005; Iacobucci et al., 2003; Memon et al., 2005; Seible et al., 1997). Columns with longer lap splice lengths have been shown to perform better. Tests on circular columns with a $35d_b$ lap splice have demonstrated relatively ductile performance, with displacement ductility levels of up to 4 being reported (Coffman et al., 1993;

Stapleton et al., 2005). Many existing bridge columns in Washington State include lap splices of the column longitudinal reinforcement with a lap length of $35d_b$.

Harries et al. (2006) conducted an experimental study on full-scale building columns incorporating a $22d_b$ lap splice at the base of the columns. In this study, all unretrofitted specimens showed poor performance with a rapid loss of stiffness and strength. Even the column without a lap splice failed at a displacement ductility level of 2.5 times the yield displacement. Columns retrofitted with external CFRP jackets showed improved ductility capacity. However, the improvement in displacement ductility capacity was limited by the onset of bar slippage in the lap splice. Research by Seible et al. (1997) has shown that slippage of lapped bars can be expected when transverse strain levels reach between 0.001 and 0.002.

Harajli et al. (2008) carried out tests on full-scale columns incorporating a $30d_b$ lap splice at the base of the columns. The tested specimens showed a loss of lateral load resisting capacity and considerable stiffness degradation in the first few cycles following bond failure. The columns tested by Harajli et al. (2008) incorporated reinforcing bars with a yield strength of 82 ksi (565 MPa), which is approximately twice the yield strength of Grade 40 reinforcing bars commonly used in older bridges in the U.S.

Several other factors also influence the performance of deficient columns. Columns under high axial load levels will fail at low lateral displacements with a significant loss of strength and stiffness (Ghosh et al., 2007; Memon et al., 2005). Other critical parameters that facilitate degradation of the lap splice are high longitudinal reinforcement ratio, large bar size, high yield strength of longitudinal reinforcement,

small spacing between vertical bars, and inadequate concrete cover (Priestley et al., 1996).

COLUMN RETROFITTING

The ability of structures to achieve adequate deformation capacity plays a significant role in the prevention of structural failures in seismic events. Ductile structures dissipate more energy and thereby may be designed for lower lateral loads than brittle structures. The deformation capacity of existing bridges can be enhanced by modifying certain substructure elements and connections. Bridge columns are typically retrofitted to increase the overall ductility of the bridge.

The performance of seismically vulnerable bridge columns can be upgraded using various techniques including reinforced concrete jacketing, steel jacketing, active confinement by prestressing wire, and composite fiber/epoxy jacketing. Of these techniques, steel jacketing is the most widely used method to retrofit bridge columns (FHWA, 2006).

Steel Jacketing

Previous research studies (Chai et al., 1991; Priestley and Seible, 1991) have shown that steel jacketing is an effective retrofit technique for seismically-deficient concrete columns. Based on satisfactory laboratory results, steel jackets have been employed to retrofit both circular and rectangular columns around the world. For circular columns, two half circle steel shells, which have been rolled to a radius equal to the column radius plus ½ in. (13 mm) to 1 in. (25 mm) for clearance, are positioned over the

portion of the column to be retrofitted, and the vertical seams are then welded (FHWA, 2006). The space between the jacket and the column is flushed with water and then filled with a pure cement grout. To avoid any significant increase in the column flexural strength, a gap of approximately 2 in. (50 mm) is typically provided between the end of the jacket and any supporting member (e.g., footing, cap beam, or girders) since at large drift angles the jacket can act as a compression member as it bears against the supporting members (Chai et al., 1990; FHWA, 2006; Priestley et al., 1996).

When the column cross section is rectangular, a rectangular steel jacket will be effective for enhancing the shear resisting capacity. However, for rectangular columns lacking proper confinement and with lap splices at the base of the columns, the rectangular cross section is often modified into oval/elliptical shape before a steel jacket is applied using similar procedures as for circular columns (Chai et al., 1990; FHWA, 2006; Priestley et al., 1996). Detailed design guidelines for steel jacketing can be found in the FHWA *Seismic Retrofitting Manual for Highway Structures* (2006).

Composite Material Retrofitting

Recent developments in the manufacturing of fiber reinforced polymer (FRP) composite materials have made these materials available for a wide range of applications, including seismic retrofit of reinforced concrete columns. Compared to steel and concrete jacketing, FRP wrapping has several advantages, including extremely low weight-to-strength ratios, high elastic moduli, resistance to corrosion, and ease of application. In addition, unidirectional FRP wrapping can improve column ductility without

considerable stiffness amplification, thereby maintaining the bridge dynamic properties (Haroun et al., 2005).

Commonly employed FRP composite materials are carbon fiber reinforced polymer (CFRP), glass fiber reinforced polymer (GFRP) and aramid fiber reinforced polymer (AFRP). Most FRP materials exhibit nearly linear elastic behavior up to failure. In general, CFRP has a higher modulus of elasticity than AFRP and GFRP. In terms of tensile strength, CFRP has the highest strength, followed by AFRP and GFRP. Despite GFRP's lower mechanical properties, it is preferable for many civil engineering applications due to its lower cost (ACI 440, 2006; Xiao et al., 2003). However, the durability of GFRP is a concern for applications in wet environments, such as that of Western Washington. The *WSDOT Bridge Design Manual M 23-60* (2006) recommends using CFRP to retrofit bridge columns in Washington since it is less affected by moisture.

FRP retrofit systems can be effective for both circular and rectangular columns. Circular jackets provide the column with a continuous confinement pressure, while rectangular jackets only provide confinement pressure at the corners. As illustrated in Figure 1, rectangular jackets rely on arching action for confinement; thus, only a portion of the cross section is effectively confined (Lam et al., 2003; Maalej et al., 2003). In order to avoid stress concentrations at the corners, rectangular columns are typically rounded prior to retrofitting (Seible et al., 1995).

The California Department of Transportation (Caltrans) funded several research studies carried out at University of San Diego to develop design guidelines for FRP retrofit systems. The findings and recommendations of these investigations are given in *Suggested Revision to Caltrans Memo to Designers 20-4 to Cover Fiberglass/Epoxy*

Retrofit of Columns (SEQAD 1993), ACTT-95/08 (Seible et al., 1995) and Priestley et al., 1996. These documents present similar design equations with only minor differences. The FHWA's *Seismic Retrofitting Manual for Highway Structures* (2006) has adopted these design guidelines for application to circular columns.

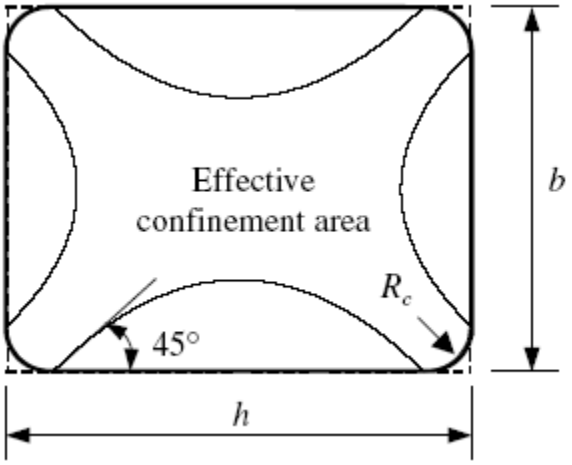

Figure 1 Effectively Confined Concrete in a Rectangular Column (Lam et al., 2003)

Caltrans primarily uses steel jacketing to retrofit deficient columns, with composite fiber wrapping listed as an alternative. Composite material retrofitting is approved only for cases that have been verified through experimental testing. The Caltrans *Memo to Designers 20-4* (1996) limits composite material retrofitting of rectangular columns to columns with cross-sectional aspect ratios of 1.5 or less and a maximum dimension of 3 ft (0.3 m). Other restrictions include axial dead load not more than 15% of the column capacity, longitudinal reinforcement ratios of 2.5% or less, and a maximum displacement ductility demand of 3. The guideline also stipulates that rectangular columns with lap splices in a potential plastic hinge region must not be retrofitted with composite fiber unless slippage of reinforcing bars is allowed.

ACTT-95/08 provides design equations to determine the required jacket thickness for each mode of failure (i.e., shear failure, confinement failure and lap splice failure) (Seible et al. 1995). Each failure mode affects different regions of the column and each of these regions needs to be evaluated. Figures 2 and 3 define these regions for columns subjected to single bending and double bending, respectively. In these figures:

L_s = lap splice length;
L_{c1} = primary confinement region for plastic hinge;
L_{c2} = secondary confinement region for plastic hinge;
L_{vi} = shear region inside plastic hinge; and
L_{vo} = shear region outside plastic hinge.

The shear strength of the FRP wrapped columns can be calculated as follows:

$$V = V_C + V_{FRP} + V_S \qquad \text{(Equation 1)}$$

Where V_C is the shear strength of the concrete, V_{FRP} is the contribution of FRP to the shear strength and V_S is the contribution of the transverse reinforcement. The contribution of the FRP can be calculated using Equation 2:

$$V_{FRP} = 2 f_{jd} t_j D \cot\theta \qquad \text{(Equation 2)}$$

In Equation 2, t_j is the thickness of the FRP, D is the column dimension in the loading direction, and θ is the inclination of the shear crack or principal compression strut. The design stress level for the jacket, f_{jd}, is calculated to be less than the ultimate stress capacity of the composite material, f_{ju}, due to limitations imposed by the concrete. When the dilation strain in the concrete exceeds 0.004, the contribution of the concrete to the shear capacity, V_C, decreases due to aggregate interlock degradation (Priestley et al., 1996). As shown in Equation 3, the design stress of the FRP, f_{jd}, is therefore determined

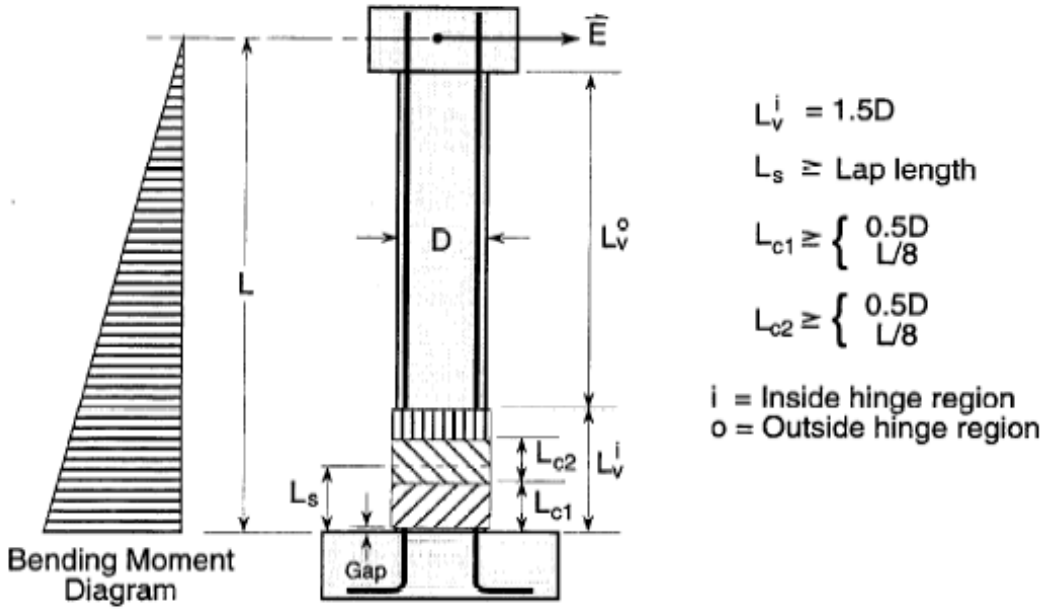

Figure 2 Single Bending Retrofit Regions (Seible et al., 1995)

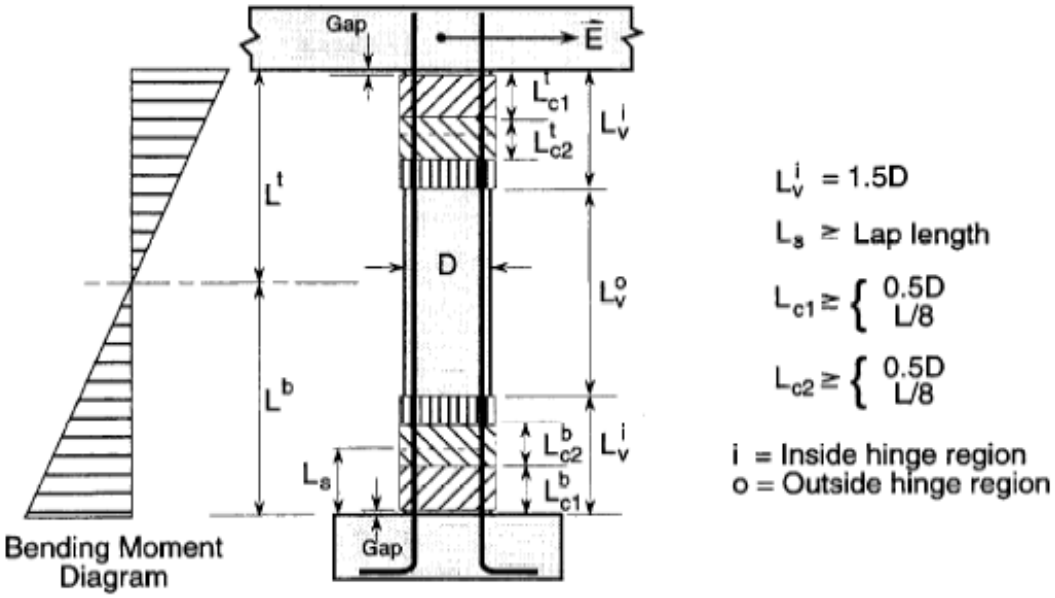

Figure 3 Double Bending Retrofit Regions (Seible et al., 1995)

using an allowable strain of 0.004.

$$f_{jd} = 0.004E_j \qquad \text{(Equation 3)}$$

In this equation, Ej is the elastic jacket modulus in the hoop direction. After simplifying the previous equations, the required jacket thickness can be calculated as follows:

$$t_j = \frac{\frac{V_o}{\phi} - (V_c + V_S)}{2 f_{jd} D \cot\theta} \qquad \text{(Equation 4)}$$

V_o can be estimated as 1.5 times the shear capacity of the column of the original column at a displacement ductility level, μ_Δ, of 1.0, and ϕ is taken as 0.85 (Seible. et al., 1995).

ACI 440 (2006) uses similar equations but with additional safety factors. The design stress of the FRP, f_{jd}, should not exceed $0.75\varepsilon_{ju}E_j$, where ε_{ju} is the ultimate strain of the FRP and E_j is the modulus of elasticity of the FRP jacket. Beside the shear strength reduction factor, ϕ, ACI 440 (2006) imposes an additional safety factor of 0.95 on the contribution of the FRP to the shear strength, V_{FRP}, to account for loss of strength through time.

For flexure-controlled columns, the level of confinement provided by the FRP jacket must meet two requirements. First, it must increase the concrete's ultimate compression strain, ε_{cu}, in order to enhance the inelastic rotation capacity and reach the desired level of ductility. Second, the FRP must prevent buckling of the longitudinal reinforcement.

FRP retrofit design for confinement of rectangular columns uses an equivalent circular column approach to utilize the design guidelines that have been developed for circular columns. The equivalent circular column diameter, D_e, is calculated from an oval jacket dimensions that may be provided to enhance confinement as shown in Figure 4. In

cases where oval jackets are not able to be provided, it is recommended to use twice the jacket thickness required for an oval jacket due to the lower efficiency of rectangular jackets (Seible et al., 1995). The equivalent circular column diameter, D_e, can be calculated using Equations 5 through Equation 9.

$$k = \left(\frac{A}{B}\right)^{2/3} \quad \text{(Equation 5)}$$

$$a = kb \quad \text{(Equation 6)}$$

$$b = \sqrt{\left(\frac{A}{2k}\right)^2 + \left(\frac{B}{2}\right)^2} \quad \text{(Equation 7)}$$

$$R_1 = \frac{b^2}{a} \text{ and } R_3 = \frac{a^2}{b} \quad \text{(Equation 8)}$$

$$D_e = R_1 + R_3 \quad \text{(Equation 9)}$$

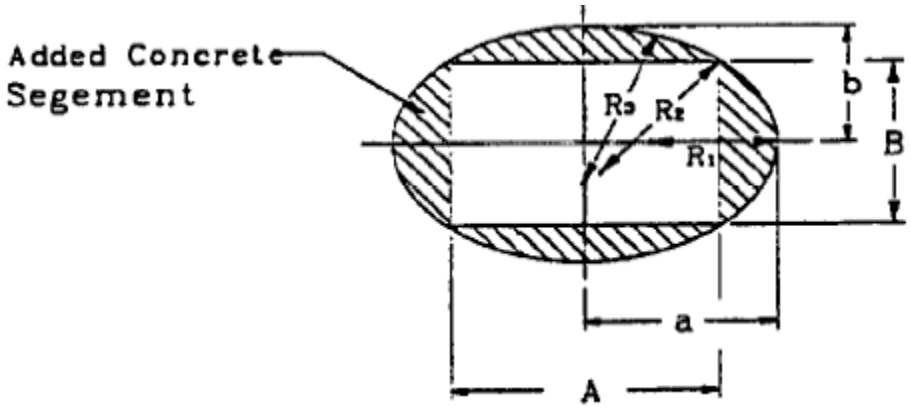

Figure 4 Oval FRP Jacket (Seible et al., 1995)

When designing the jacket, the required ultimate compression strain is calculated based on the desired ductility level. The design jacket thickness required to increase the ultimate concrete compression strain depends on the relationship between ultimate strain, ε_{cu}, and the level of confinement. The required jacket thickness to enhance confinement can be calculated using Equations 10 through Equation 14.

$$L_p = 0.08L + 0.022 f_{sy} d_b \qquad \text{(Equation 10)}$$

L_p is the length of the plastic hinge, L is the distance to the contra-flexure point measured from the end of the column, d_b is the diameter of longitudinal bars and f_{sy} is the yield strength of longitudinal reinforcement.

For a given displacement ductility, μ_Δ, the ultimate curvature, ϕ_u, can be obtained from the following two equations:

$$\mu_\Delta = 1 + 3(\mu_\phi - 1)\frac{L_p}{L}\left(1 - 0.5\frac{L_p}{L}\right) \qquad \text{(Equation 11)}$$

$$\mu_\phi = \frac{\phi_u}{\phi_y} \qquad \text{(Equation 12)}$$

ϕ_y is determined from a moment-curvature analysis of the section. From geometry, ε_{cu} is then computed using Equation 13.

$$\varepsilon_{cu} = \phi_u c_u \qquad \text{(Equation 13)}$$

The jacket thickness can be then designed as follows:

$$t_j = 0.09\frac{D_e(\varepsilon_{cu} - 0.004) f'_{cc}}{f_{ju}\varepsilon_{ju}} \qquad \text{(Equation 14)}$$

In Equation 14, f_{ju} is the ultimate strength of the fiber and ε_{ju} is the strain of the fiber at failure. f'_{cc} is the compression strength of the confined concrete and can conservatively be taken as 1.5f '$_c$ (Seible et al 1995).

For slender columns, the amount of FRP needed to prevent buckling must be checked. The jacket thickness, t_j, required to prevent buckling can be calculated as follows:

$$t_j = \left(\frac{nD_e}{E_j}\right) ksi \text{ or } t_j = \left(\frac{nD_e}{E_j}\right) MPa \qquad \text{(Equation 15)}$$

In Equation 15, n is the number of longitudinal bars and E_j is the modulus of elasticity of the jacket in ksi.

Lap splice design guidelines are based on a simplified mechanism of failure. The mechanism assumes that a series of cracks in a vertical plane occurs due to a relative slippage of rebars and movement of longitudinal bars relative to the core concrete, as shown in Figure 5 (Priestley et al., 1996). Applying an external clamping force increases the frictional force along the cracked surfaces limiting bar slippage as well as concrete cover spalling.

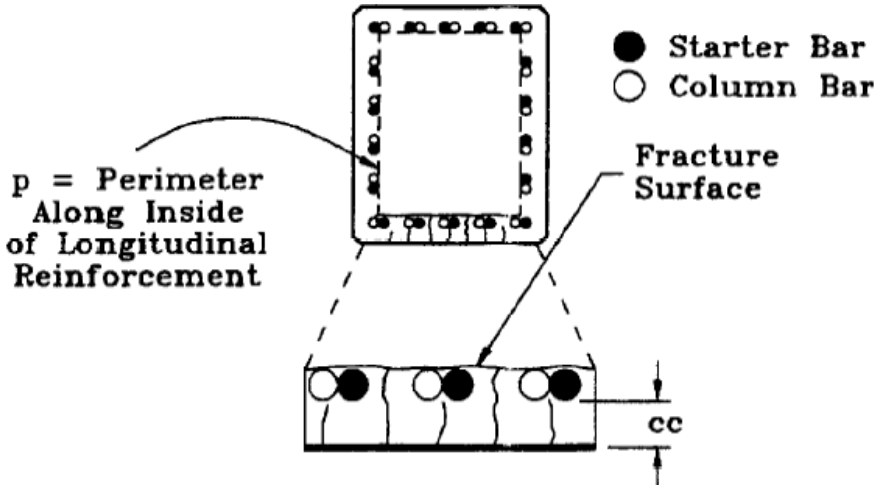

Figure 5 Lap Splice Failure Model (Priestley et al., 1996)

Tests have indicated that debonding starts at transverse strains ranging from 0.001 to 0.002. A jacket strain limit of 0.001 is therefore proposed for design (Seible et al., 1995). Assuming the coefficient of friction, μ, for concrete cracks is 1.4, the oval jacket thickness required to prevent bond failure can be calculated as follows:

$$t_j = 500\frac{D_e\left(f_l - f_h\right)}{E_j} \qquad \text{(Equation 16)}$$

In Equation 16, f_h, the confining pressure of the transverse reinforcement, is 0 for columns with low transverse reinforcement ratios, and f_l is the lateral clamping pressure over the lap splice, which can be determined using Equation 17.

$$f_l = \frac{A_s f_{sy}}{\left[\frac{p}{2n} + 2(d_b + cc)\right] L_s} \qquad \text{(Equation 17)}$$

In Equation 17, p is the perimeter line in the column cross section along the lap-spliced bar locations, n is the number of spliced bars along p, cc is the cover concrete thickness, and A_s is the area of a vertical bar with diameter d_b.

Similar to the plastic hinge design, the design equations for lap splice confinement are based on circular cross-sections. For rectangular cross-sections, it is recommended that an elliptical concrete shell be placed around the column. If a rectangular jacket is used, it is recommended to use double the amount of the FRP required for an oval section (Seible et al., 1995). Rectangular jackets installed over rectangular columns can be effective only if controlled debonding is permissible (Seible et al 1995).

EXPERIMENTAL TESTING PROGRAM

TEST SPECIMENS AND PARAMETERS

The test specimens of this study were constructed to be representative of rectangular bridge columns present in Washington State. Design plans of Washington State bridge columns from the 1950's and 1960's were reviewed to obtain information about older design and construction practices. Based on the bridge plan reviews along with recommendations from the Washington State Department of Transportation

(WSDOT) and the Federal Highway Administration (FHWA), typical column details were chosen to reveal potential modes of failures in older columns.

The experimental tests were conducted on 40% (1:2.5) scale specimens which modeled the prototype dimensions, reinforcing ratios and detailing, and material properties. The specimens incorporated lap splices at the base of the columns and deficient transverse reinforcement. Shear deficiencies were not considered in this study. Test objectives include evaluating the performance of specimens representing the as-built conditions, assessing the improvements achieved by various retrofitting techniques (i.e., FRP wrapping and steel jacketing), and investigating the effect of cross-sectional aspect ratio on retrofit performance.

A summary of the test specimens is given in Table 1. A total of eight specimens was tested. Seven of the columns were built identically, with a cross-sectional aspect ratio of 1.5, while the eighth specimen had a cross-sectional aspect ratio of 2. All specimens had an approximate longitudinal reinforcement content of 1.2%, provided using No. 4 Grade 40 rebar, and ¼-in. (6.3-mm) diameter smooth mild steel hoops at 5 in. (12.5 mm) on center for the transverse reinforcement. The column longitudinal bars were lap spliced at the base of the column to starter bars extending up from the foundation. The length of the lap splice was 35 times the column longitudinal bar diameter (d_b). The footings were oversized to force failure of the specimen into the columns.

Two specimens were tested without any retrofitting in order to evaluate the performance of the as-built columns. The bottom section of all other columns was retrofitted. One specimen was retrofitted with oval steel jacket while the remaining five

specimens were retrofitted using CFRP wrapping. Details of the various retrofit measures are discussed along with the test results later in this report.

Table 1 Summary of Test Specimens

Specimen	Test Parameter	Cross-section Aspect Ratio	Retrofit
AB-1	Control	1.5	None
AB-2	Control	1.5	None
SJ	Steel jacket – oval	1.5	Oval –shaped steel jacket
FRP-MS	CFRP - oval	1.5	Oval-shaped CFRP jacket
FRP-4	CFRP - rectangular	1.5	Rectangular CFRP jacket
FRP-6	CFRP amount	1.5	Rectangular CFRP jacket
FRP-8	CFRP amount	1.5	Rectangular CFRP jacket
AR-2	Aspect ratio	2	Rectangular CFRP jacket

All specimens were constructed using concrete with an average measured compressive strength of 4500 psi (31 MPa) at the time of testing. The grout used for the column retrofit jackets had an average compressive strength of 6500 psi (45 MPa), measured at the time of testing. The longitudinal steel was Grade 40 with average measured yield strength of 48 ksi (331 MPa). Mild steel with a measured yield strength of 54 ksi (372 MPa) was used for the transverse reinforcement. The steel jacket used for retrofitting was rolled from 0.185-in. (4.7-mm) thick steel plate with a specified yield strength of 36 ksi (248 MPa). The uniaxial CFRP sheet used for retrofitting had a specified elastic modulus E_f = 10,100 ksi (69,637 MPa), a specified ultimate tensile strength f_{uf} = 140 ksi (965 MPa), and a nominal thickness t_f = 0.05 in. (1.27 mm).

TEST SETUP AND PROCEDURES

The overall test setup is shown in Figures 6 and 7. The specimens were subjected to reverse cyclic lateral loading through increasing levels of lateral displacements. To simulate the dead load on bridge columns, 7% of the column axial capacity ($0.07f'_cA_g$) was applied as an axial load using a hydraulic jack mounted on a low-friction trolley. The lateral load was applied using a horizontally-aligned 100-kip (445-kN) hydraulic actuator.

Loading of the test specimens was slowly applied in a quasi-static manner. The horizontal loads were applied under displacement control based on a pattern of progressively increasing displacements, referenced to the horizontal displacement to cause first yield (Δ_y) in the column. The loading pattern for the specimens consisted of three cycles at displacement levels of ±0.5, ±1, ±1.5, ±2, ±2.5, ±3, ±4, ±6, ±8, ±10, and ±12 times Δ_y , unless failure occurred first. Failure was defined as a 20% drop in peak lateral load for each specimen. Δ_y was theoretically determined from moment-curvature analyses. For the specimens with an aspect ratio of 1.5, the estimated Δ_y was 0.4 in. (10 mm.); for the specimen with an aspect ratio of 2, the estimated Δ_y was 0.3 in. (7.6 mm).

Load and displacement data were collected at 1-second intervals from the actuator load cell, displacement potentiometers and strain gages. Potentiometers and load cells measured column displacements and applied loads, respectively. Potentiometers were also placed on the top of the footing and extended to reference points along the height of the column to determine column rotations. Strain gages were used to monitor the strains in the column longitudinal bars, transverse reinforcement and applied retrofits.

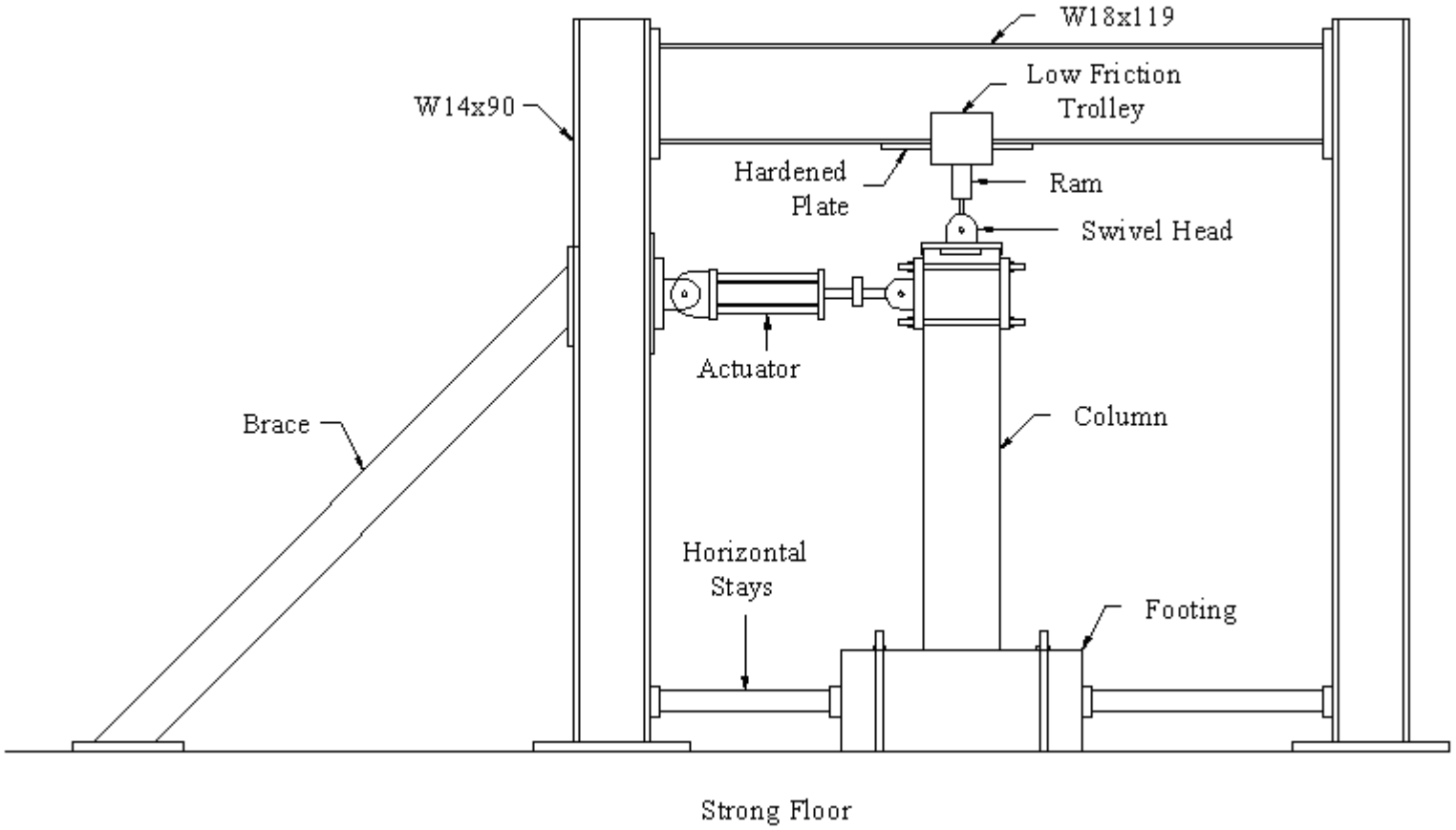

Figure 6 Test Setup

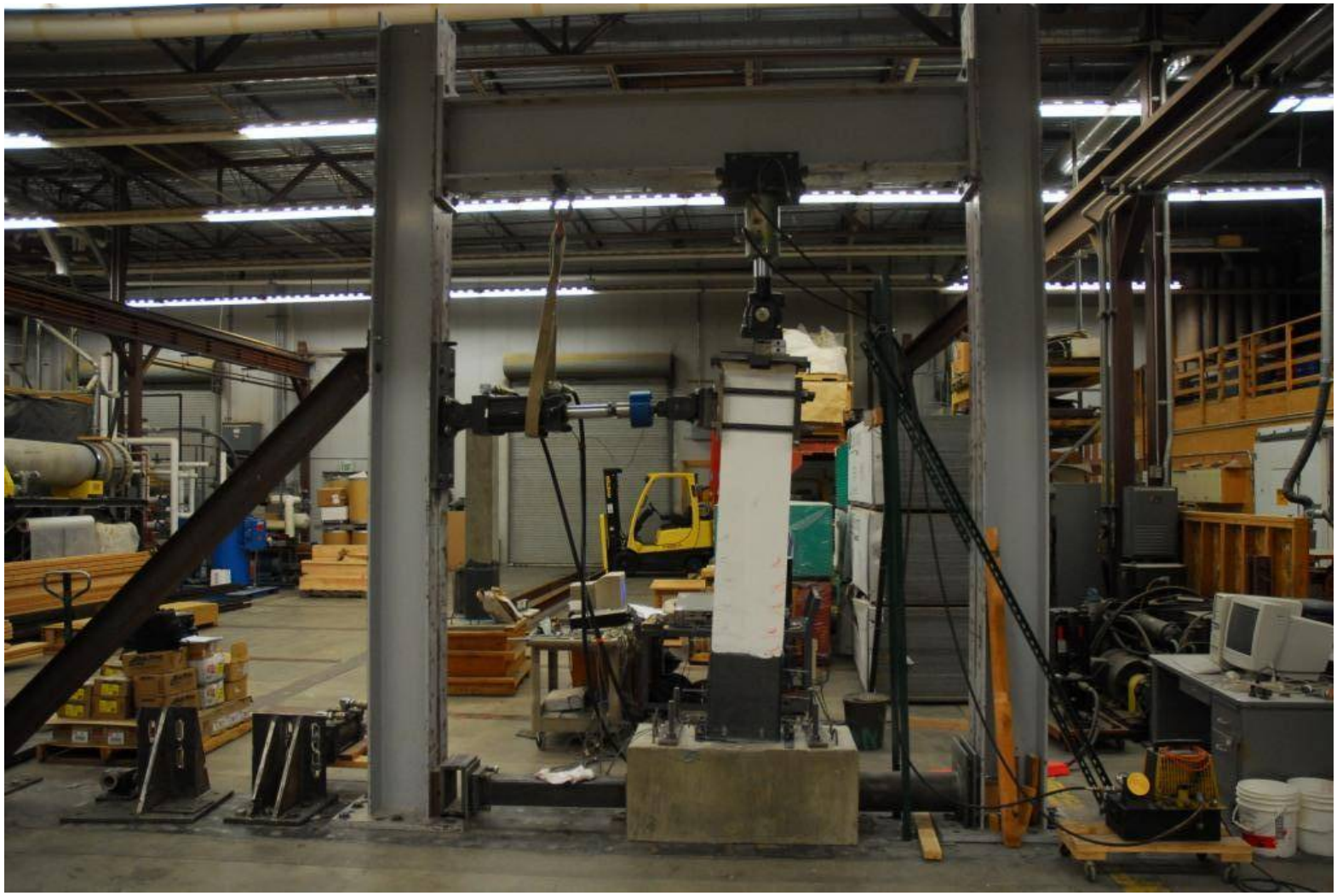

Figure 7 Photograph of the Test Setup

TEST RESULTS AND DISCUSSION

In this section, results of the experimental tests are summarized. For each specimen, details of the column specimen and, if applicable, retrofit design are discussed. The seismic performance of each specimen was evaluated based on failure mode, displacement ductility, and hysteretic behavior. Displacement ductility, μ_Δ, is the ratio of the measured lateral displacement at failure, defined as a 20% drop in peak load, to the measured yield displacement. The measured yield displacement was determined by fitting a bilinear load-displacement relationship to the envelope of the experimentally-obtained hysteretic curves, as outlined by Priestley et al. (1996). The energy dissipation of each specimen was determined by calculating the area under the load-displacement hysteresis curves.

For reference in the results discussion, reported positive displacements are associated with displacing the column in the northerly direction, and reported positive lateral loads are associated with pushing of the column in the northerly direction.

More detailed discussion of the results is given by Endeshaw (2008).

AS-BUILT SPECIMENS

Specimens AB-1 and AB-2 were designed to be representative of as-built conditions with deficient transverse reinforcement and a $35d_b$ lap splice at the base of the column. Details of the as-built specimens are given in Figure 8. The performance of these specimens was intended to reveal vulnerabilities in the existing columns and to establish benchmarks to evaluate the effectiveness of the applied retrofit measures.

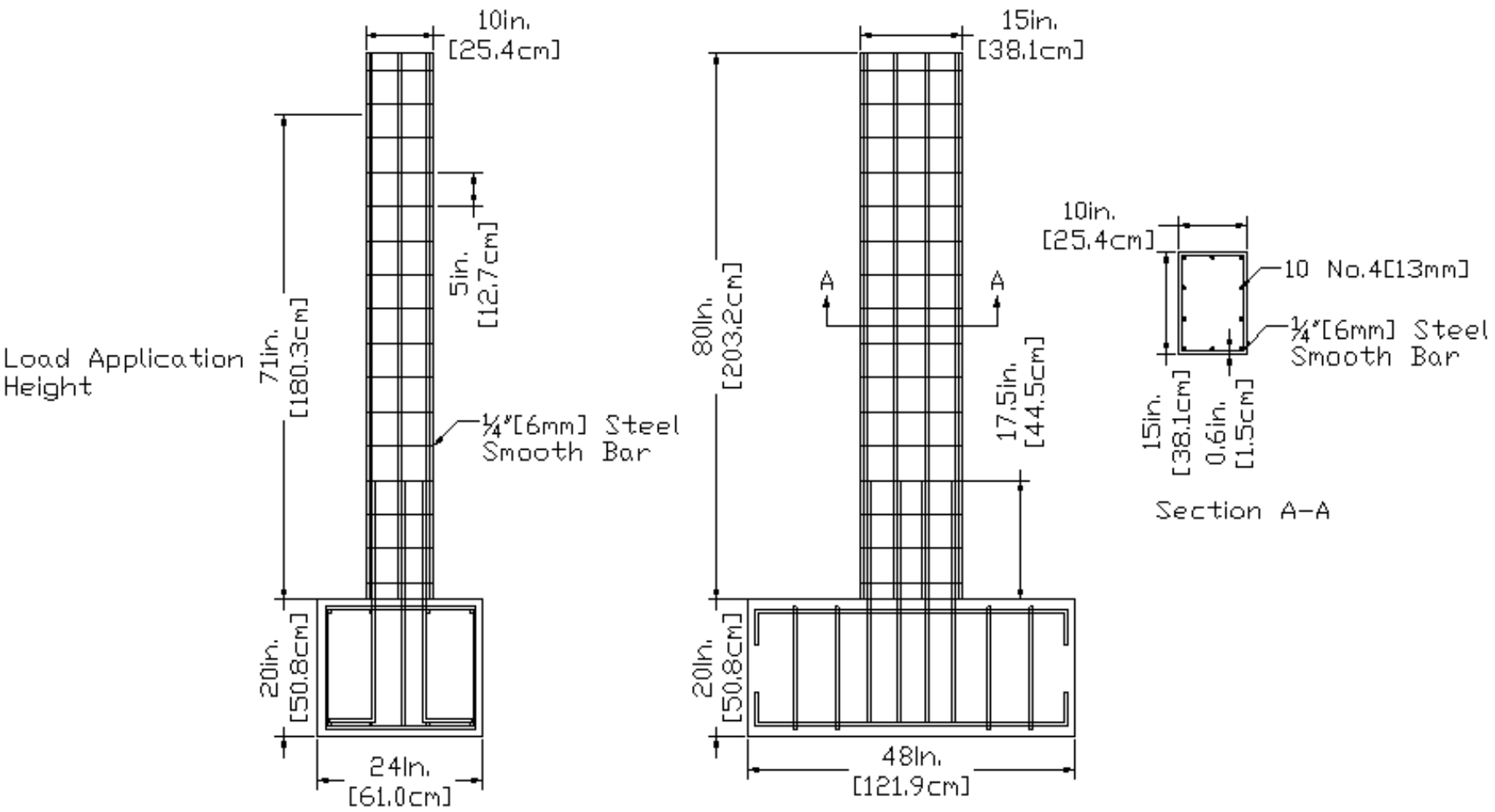

Figure 8 Details of As-built Specimens

Specimen AB-1

The lateral load vs. displacement hysteresis curves for Specimen AB-1 are shown in Figure 9 and indicate reasonable ductility and energy dissipation. Specimen AB-1 was able to attain a maximum displacement ductility, μ_Δ, of 6.4.The peak lateral load was 17 kips (75 kN) and occurred at a lateral displacement of approximately 2.4 in. (61 mm). The specimen exhibited a significant decrease in lateral strength at a displacement level of 3.2 in. (81 mm), and the applied load dropped below 80% of the peak load during the second cycle at this displacement level. The stiffness of the column showed minor degradation up to the displacement level of 1.6 in. (30 mm). The last two displacement levels (i.e., 2.4 in. (61 mm) and 3.2 in. (81 mm)) displayed a more pronounced loss of stiffness. At the end of testing, the specimen was still capable of sustaining the applied axial load.

Most of the damage in this column occurred at the base of the column. However, numerous flexural cracks, visible under applied loading, were observed up to the mid-height of the column (see Figure 10). The first horizontal flexural crack was noticed at a displacement of 0.6 in. (15 mm), and the formation of flexural cracks continued with increasing levels of displacements. The concrete cover over the lap splice showed only minimal signs of vertical cracking. At a displacement of 1.2 in. (30 mm), spalling of the concrete cover at the base of the column began due to flexural loading, exposing the column reinforcement. Once the concrete cover was lost, the longitudinal bars in this region began to buckle. Figure 11 shows a buckled longitudinal bar at a displacement level of 2.4 in. (61 mm). During the last loading cycle (i.e., the second cycle of the 3.2 in. (81 mm) displacement level), a “popping” sound was heard when one of the longitudinal

bars ruptured due to a low-cycle fatigue failure, as shown in Figure 12. The rupture also produced a "kink" in the lateral load vs. displacement hysteresis curves, as shown in Figure 9.

The strain levels in the starter bars, longitudinal bars and the bottom transverse hoop were monitored during testing. Yielding of the reinforcement occurred at all monitored locations. The maximum tensile strain in the starter bars exceeded the strain gage capacity of 10,000 x 10^{-6} strain (microstrain), and the strain gages were lost towards the end of the test. The bottom hoop also experienced high levels of strains that caused the strain gages to fail after the strain gage capacity was exceeded.

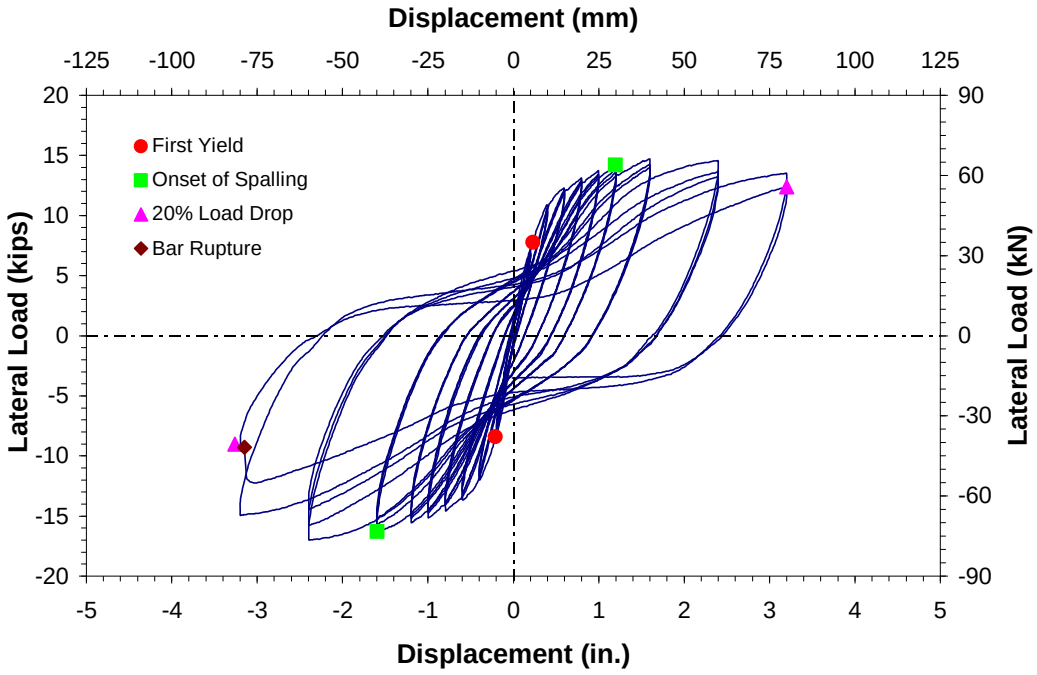

Figure 9 Lateral Load vs. Displacement Hysteresis Curves for Specimen AB-1

Figure 10 Specimen AB-1 After Testing

Figure 11 Buckled Longitudinal Reinforcement of Specimen AB-1

Figure 12 Ruptured Longitudinal Reinforcement of Specimen AB-1

Specimen AB-2

The detailing of Specimen AB-2 was identical to that of Specimen AB-1. The lateral load vs. displacement hysteresis curves for Specimen AB-2 are shown in Figure 13. Similar to Specimen AB-1, Specimen AB-2 reached a displacement ductility of 6.4 while still able to carry the applied axial load. However, Specimen AB-2 developed vertical cracks at the base of the column associated with lap splice failure during testing. The hysteresis curves for Specimen AB-2 were similar to those for Specimen AB-1. The peak lateral load was 16.1 kips (72 kN) and occurred at a lateral displacement of approximately -2.4 in. (61 mm). Failure in Specimen AB-2 occurred while loading to a

displacement of +3.2 in. (81 mm). Significant loss in stiffness occurred at displacement levels of 2.4 in. (61mm) and 3.2 in. (81 mm).

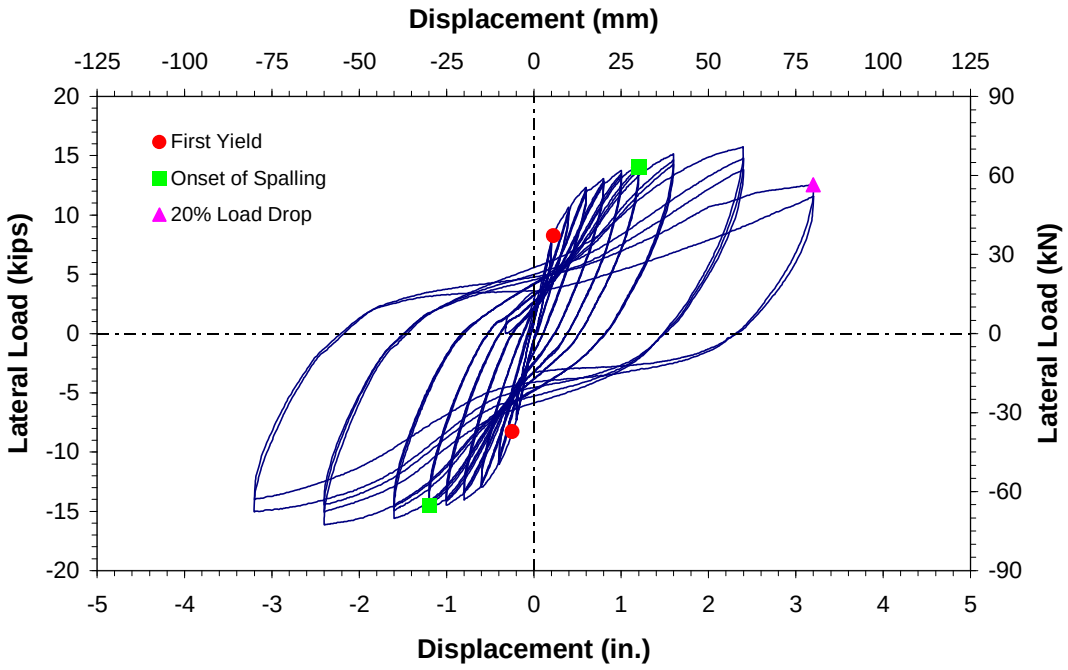

Figure 13 Lateral Load vs. Displacement Hysteresis Curves for Specimen AB-2

Horizontal-flexure cracks started to develop at the extreme faces of the column, in the direction of loading, while cycling at a displacement level of 0.6 in. (15 mm). At the end of the test, a number of small flexural cracks covered the bottom half of the column. Vertical cracks associated with lap splice failure began to form at the base of the column while cycling at a displacement level of 1 in. (25 mm). These cracks continued to propagate with increasing levels of lateral displacements. The most notable vertical crack, which occurred on the north face of the column, propagated to the full height of the lap splice during cycling at a displacement level of 2.4 in. (61 mm), as shown Figure 14. At this displacement level, the column reinforcement also became visible due to

spalling of the cover concrete. As shown in Figure 14, the bottom transverse hoop opened up due to the load exerted on it by the buckling longitudinal reinforcement. The south face of Specimen AB-2 performed similar to Specimen AB-1, where spalling due to flexural loading and buckling of the bar concentrated in the bottom 5 in. (127 mm), with eventual low-cycle fatigue fracture of the reinforcement on this face. A photo of the south side of the column is shown in Figure15.

The strain levels in the starter bars, longitudinal bars and the bottom transverse hoop were monitored. The readings indicated similar behavior to that of Specimen AB-1. The maximum tensile strain in the starter bars exceeded the strain gage capacity of 10,000 microstrain, and the strain gages failed towards the end of the test. The bottom hoop also experienced a high level of strain that caused the strain gages to fail due to the load exerted by the buckling of the longitudinal bars. The maximum recorded strains were beyond the yield strains of the reinforcement.

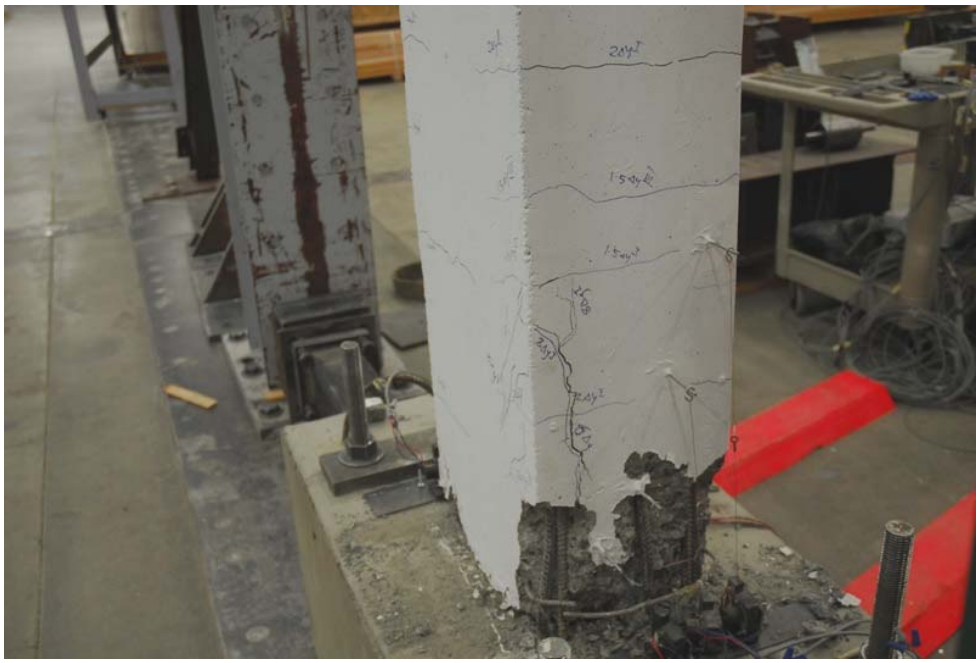

Figure 14 The North Side of Specimen AB-2 Towards the End of Testing.

Figure 15 The South Side of Specimen AB-2 Towards the End of Testing.

Summary of As-Built Specimen Tests

The lateral load vs. displacement hysteresis curves for the two as-built specimens were similar. Both specimens sustained similar peak lateral loads and failed at a displacement of 3.2 in. (81 mm). Damage in the as-built specimens occurred primarily at the base of the columns. Failure in Specimen AB-1 was a result of spalling of the concrete at the base of the column due to flexural loading, leading to buckling and eventual low-cycle fatigue fracture of the longitudinal reinforcement. Failure in Specimen AB-2 was due to a similar mechanism on the south face of the column, combined with vertical cracking leading to a lap splice failure on the north face.

Based on previous research, it was anticipated that the as-built columns would exhibit a rapid degradation of strength and stiffness due to lap splice failure. However, the tested columns exhibited reasonably good ductility and energy dissipation capacity,

and only one of the specimens experienced a lap splice failure. The superior performance of the as-built columns is likely a result of the following factors present in the column specimens of this study: a relatively long lap splice length ($35d_b$); a low axial load level ($0.07f'_cA_g$); and a low longitudinal steel reinforcement ratio ($\rho = 1.2\%$). Previous tests on circular columns with a $35d_b$ lap splice length have also shown a relatively ductile performance, achieving up to a displacement ductility level of 4 (Coffman et al., 1993; Stapleton et al., 2005). Other researchers (Ghosh et al., 2007; Memon et al., 2005) have also shown that columns under low axial load levels perform better than columns under high axial load levels. Low longitudinal reinforcement content leads to wider spacing between vertical bars, which helps the lap splice to perform better (Priestley et al., 1996). The combined effect of these factors is likely the reason for the better-than-expected performance of the as-built specimens.

Orangun et al. (1977) developed an empirical equation to predict the average bond stress of spliced bars at bond failure. This empirical bond stress equation provides the basis for the tensile development length equation in ACI 318-05 (ACI, 2005). The bond stress equation accounts for the unconfined lap splice capacity and the confinement effect from any transverse reinforcement present. For lap splices under cyclic loading, confinement from the transverse reinforcement is rapidly lost, resulting in inferior performance for cyclic loading when compared to the response under monotonic loading (Harries et al., 2006). The Orangun equation can be used to estimate the capacity of a lap splice under cyclic loading by disregarding the contribution of transverse reinforcement confinement, as given in Equation 18 (Harajli et al., 2008; Harries et al., 2006). This bond stress equation applies only for cases where the ratio of concrete cover to the bar

diameter (cc/d_b) is less than 2.5 (Orangun et al., 1977). It should be noted that a rapid degradation of the lap splice is expected once the bond stress exceeds the lap splice capacity.

$$u_{unconfined} = \left(1.2 + \frac{3cc}{d_b} + \frac{50d_b}{L_s}\right)\sqrt{f_c'} \quad \text{(psi units)}$$

$$u_{unconfined} = \left(0.1 + \frac{cc}{4d_b} + \frac{25d_b}{6L_s}\right)\sqrt{f_c'} \quad \text{(MPa units)} \qquad \text{(Equation 18)}$$

Based on this model, the bond stress capacity of the lap splices in the as-built specimens can be estimated. Using static equilibrium between the bar force and the bond force, the bond stress required to yield the lapped bars can be determined. Figure 16 shows predicted lap splice capacity, the bond stress required to yield the lapped bars, and the bond stress required to develop 1.25 times the yield strength of the lapped bars as a function of lap splice length, L_s. As shown in Figure 16, the model predicts that the as-built specimens of this study, with a $35d_b$ lap splice, will develop approximately 1.25 times the yield strength of the lapped bars. This is consistent with the results obtained from the as-built specimens tests in which lap splice failure occurred on only one side of one of the as-built specimens.

Figure 16 also shows the predicted lap splice capacity for parameters typical of those in full-scale columns: No. 11 (36 mm) bars, 1.5 in. (38 mm) cover, and a yield stress of 48 ksi. For these parameters and with a $35d_b$ lap splice, the model predicts that the lapped bars will develop their yield strength but not reach 1.25 times yield. Thus, lap splice failure may be more likely in full-scale columns than with the 40% scale test specimens.

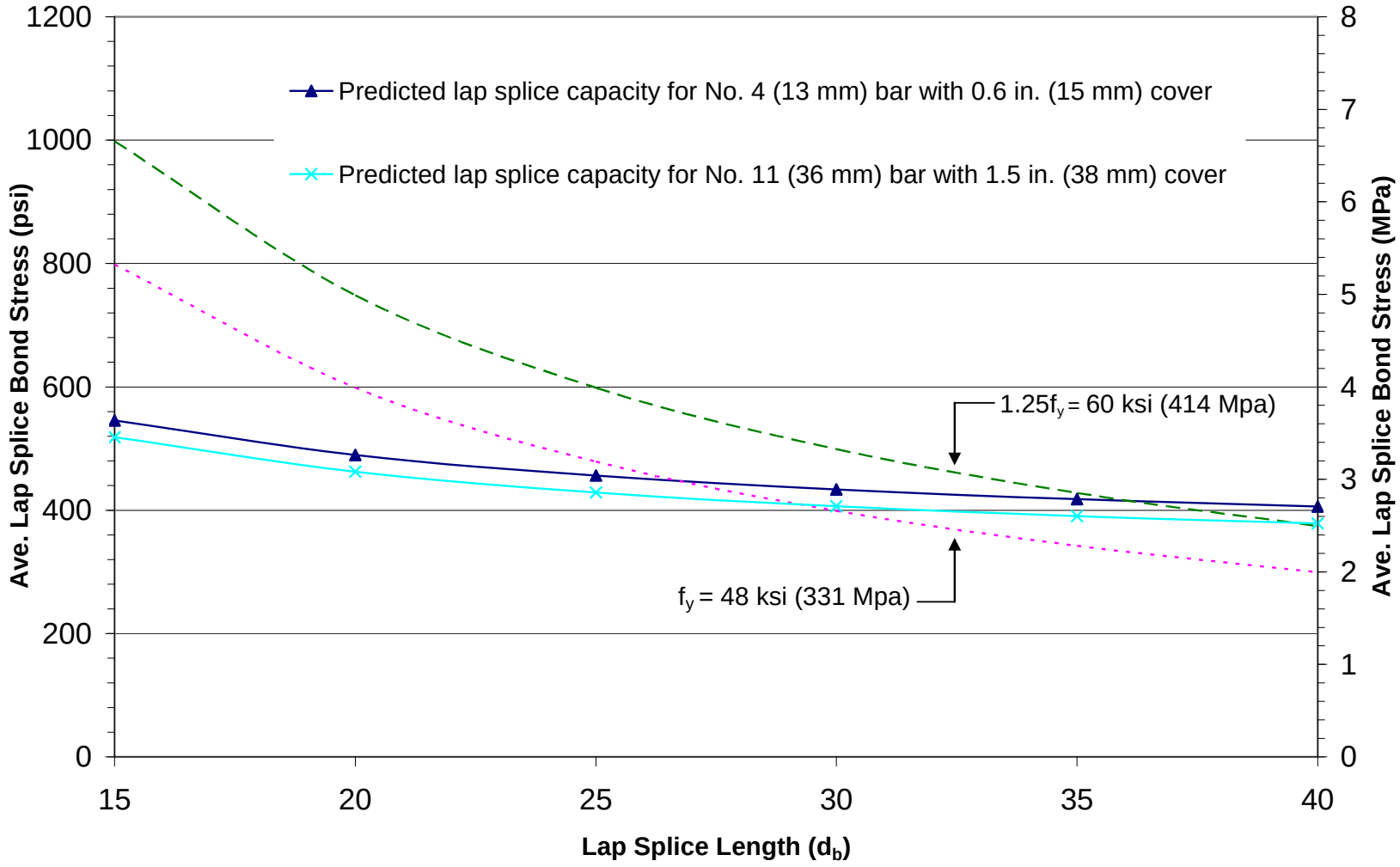

Figure 16 Lap Splice Bond Stress as a function of Lap Splice Length

Although the construction details of the tested specimens are representative of those for Washington State's interstate column inventory, the results of this study do not necessarily apply to all existing columns. As was noted, variations in axial load level and longitudinal reinforcement content will influence the performance of columns in the field. In addition, full-scale columns with larger bar sizes may be more prone to poor performance than the tested specimens due to the inability of scaled columns to accurately represent reinforcement bond and concrete cracking.

SPECIMEN RETROFITTED USING STEEL JACKETING

Specimen SJ

Specimen SJ was constructed identically to the as-built specimens, except that the specimen was retrofitted with an oval-shaped steel jacket to provide confinement over the lap splice region. The jacket was designed based on the FHWA guidelines (2006); however, a jacket thickness of 0.185 in. (47 mm) was used rather than the required thickness of 0.15 in. (38 mm) due to steel availability issues. The steel jacket was constructed from two rolled steel shells which were welded together. The steel jacket was then placed over the top of the column and positioned around the base of the column. The gap between the jacket and the column was filled with a non-shrink, high-strength grout. The jacketing was 18 in. (46 cm) high, which covered the entire lap splice region. A 1.0 in. (25 mm) gap was provided between the steel jacket and the footing to prevent the sections from bearing against each other at larger drift angles. Figure 17 provides details of the steel jacket retrofit.

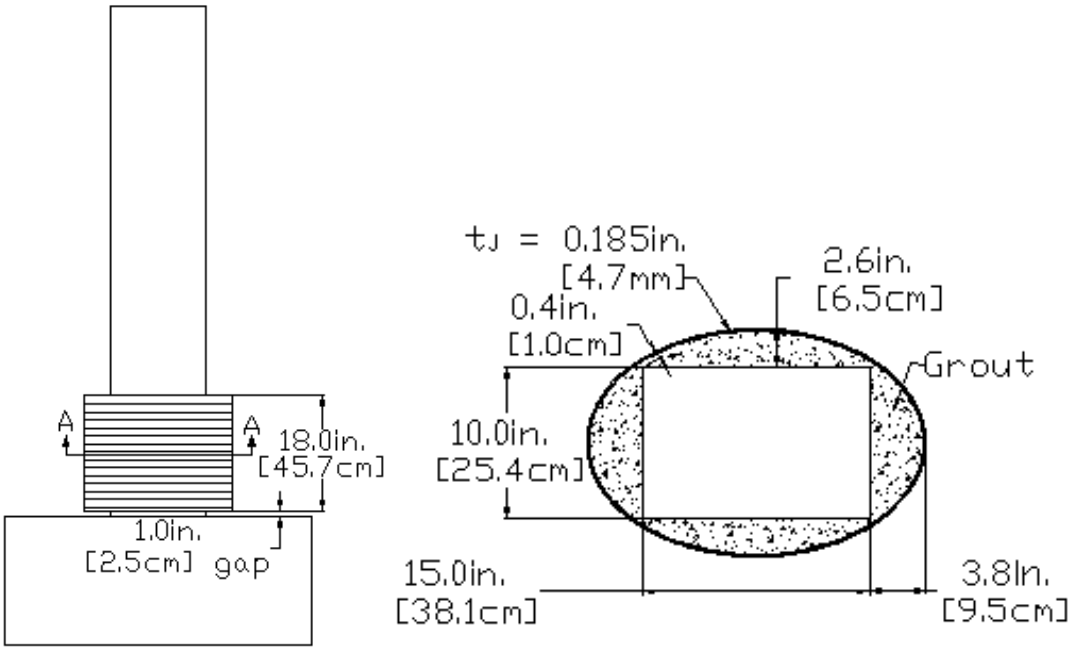

Section A-A

Figure 17 Details of the Steel Jacket Retrofit

The lateral load vs. displacement hysteresis curves for specimen SJ are given in Figure 18. Specimen SJ was able to attain a displacement ductility, μ_Δ, of 7.1 At a displacement of 2.4 in. (61 mm), the column resisted a peak lateral load of 14.5 kips (65 kN). Failure in Specimen SJ occurred while loading to the second cycle of the 3.2 in. (81 mm) displacement level. The hysteresis loops of Specimen SJ were slightly wider in comparison to those for the as-built specimens. However, the peak lateral loads resisted by Specimen SJ were slightly lower than those for the as-built specimens, possibly due to some construction irregularities. At the end of testing, the specimen was still capable of sustaining the applied axial load.

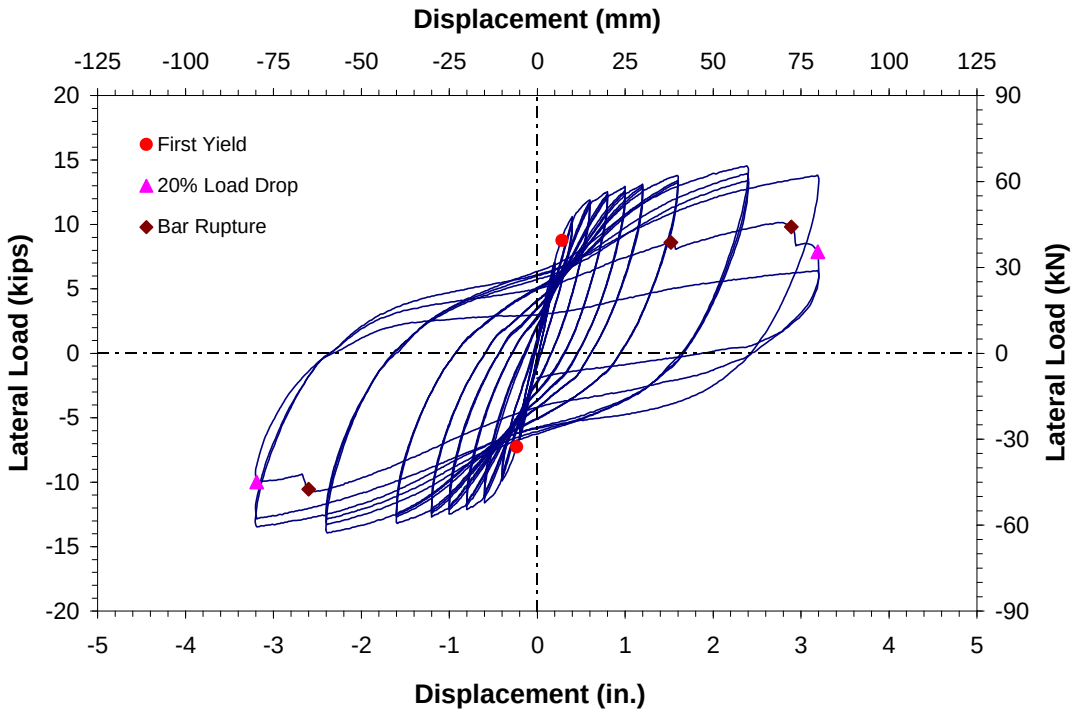

Figure 18 Lateral Load vs. Displacement Hysteresis Curves for Specimen SJ.

A photograph of Specimen SJ during testing is given in Figure 19. The behavior of Specimen SJ was dominated by hinging at the gap provided between the steel jacket and the footing. The first visible flexure crack in the gap region occurred during the first cycle at the 1.2 in. (30 mm) displacement level. There was no observable flexural cracking above the steel jacket throughout the test. The concrete within the gap region started to crush and spall during the third cycle at the 1.6 in. (41 mm) displacement level, as shown in Figure 20. At a displacement level of 3.2 in. (81 mm), buckling of the longitudinal bars within the gap was observed. During the second cycle at the 3.2 in. (81 mm) displacement level, a series of "popping" sounds accompanied by a "kink" in the lateral load vs. displacement hysteresis curves occurred due to a low-cycle fatigue fracture of the reinforcing bars. Three longitudinal bars ruptured by the end of the test.

Figure 19 Specimen SJ During Testing

Figure 20 Spalling in Specimen SJ

The strain in the starter bars, longitudinal bars, bottom transverse hoop and steel jacket were monitored during testing. The maximum tensile strain in the bottom hoop was 500 microstrain, indicating that yielding of the transverse reinforcement did not occur. The starter bars showed a high level of strain, exceeding the strain gage capacity of 10,000 microstrain. The maximum strain level in the steel jacket was 120 microstrain, less than 10% of the yielding strain for the jacket.

Summary of Steel Jacketed Specimen Test

The test results for Specimen SJ showed a ductile performance achieving a displacement level of 3.2 in. (81 mm). Specimen SJ failed due to plastic hinging in the gap provided between the jacket and the footing, leading to eventual low-cycle fatigue fracture of the reinforcement. The peak lateral load resisted by Specimen SJ was slightly smaller than that for the as-built specimens, possibly due to some misalignment of the reinforcing bars during construction. Specimen SJ attained a displacement ductility of 7.1, which is in the typical range of 6 to 8 reported for steel-jacketed columns (Seible et al., 1997). Although the applied steel jacket only modestly improved the displacement ductility in comparison to that of the as-built specimens, significantly lower strains developed in the transverse hoop reinforcement as a result of the confinement provided by the retrofit jacket.

SPECIMENS RETROFITTED USING CFRP WRAPPING

Apart from the applied retrofit, the detailing for Specimens FRP-MS, FRP-4, FRP-6 and FRP-8 was identical to that used for the as-built specimens. Specimen AR-2 was constructed with a cross-sectional aspect ratio of 2, with all other speciment parameters kept essentially the same as those for the as-built specimens. Details of Specimen AR-2 are given in Figure 21. All of these specimens were retrofitted with CFRP composite wrapping at the base of the columns.

The FRP reinforcement consisted of a unidirectional carbon fiber fabric that can be impregnated onsite with laminating resin to create a CFRP laminate. Different suppliers and FRP types were considered before choosing the one with the highest fabric areal weight density to minimize the required number of layers. The CFRP used had a fabric areal weight density of 18 oz/yd^2 (600 g/m^2). The cured laminate had a specified elastic modulus E_f = 10,100 ksi (69,637 MPa), a specified ultimate tensile strength f_{uf} = 140 ksi (965 MPa), and a nominal thickness t_f = 0.05 in. (1.27 mm).

For Specimens FRP-MS and FRP-4, the number of CFRP layers was based on recommendations provided by ACTT-95/08 (Seible et al., 1995). The number of CFRP layers installed on Specimen FRP-6 and FRP-8 were increased by 150% and 200% of ACTT-95/08's recommendations for rectangular retrofit jackets, respectively, to investigate the effects of increased CFRP thickness on the performance of the retrofitted columns. Although the ACTT-95/08 recommendations apply to rectangular columns with a cross-sectional aspect ratio of 1.5 or less, the CFRP wrapping on Specimen AR-2 was based on these recommendations in order to examine if the constraints on the cross-sectional aspect ratio contained in these guidelines could be expanded.

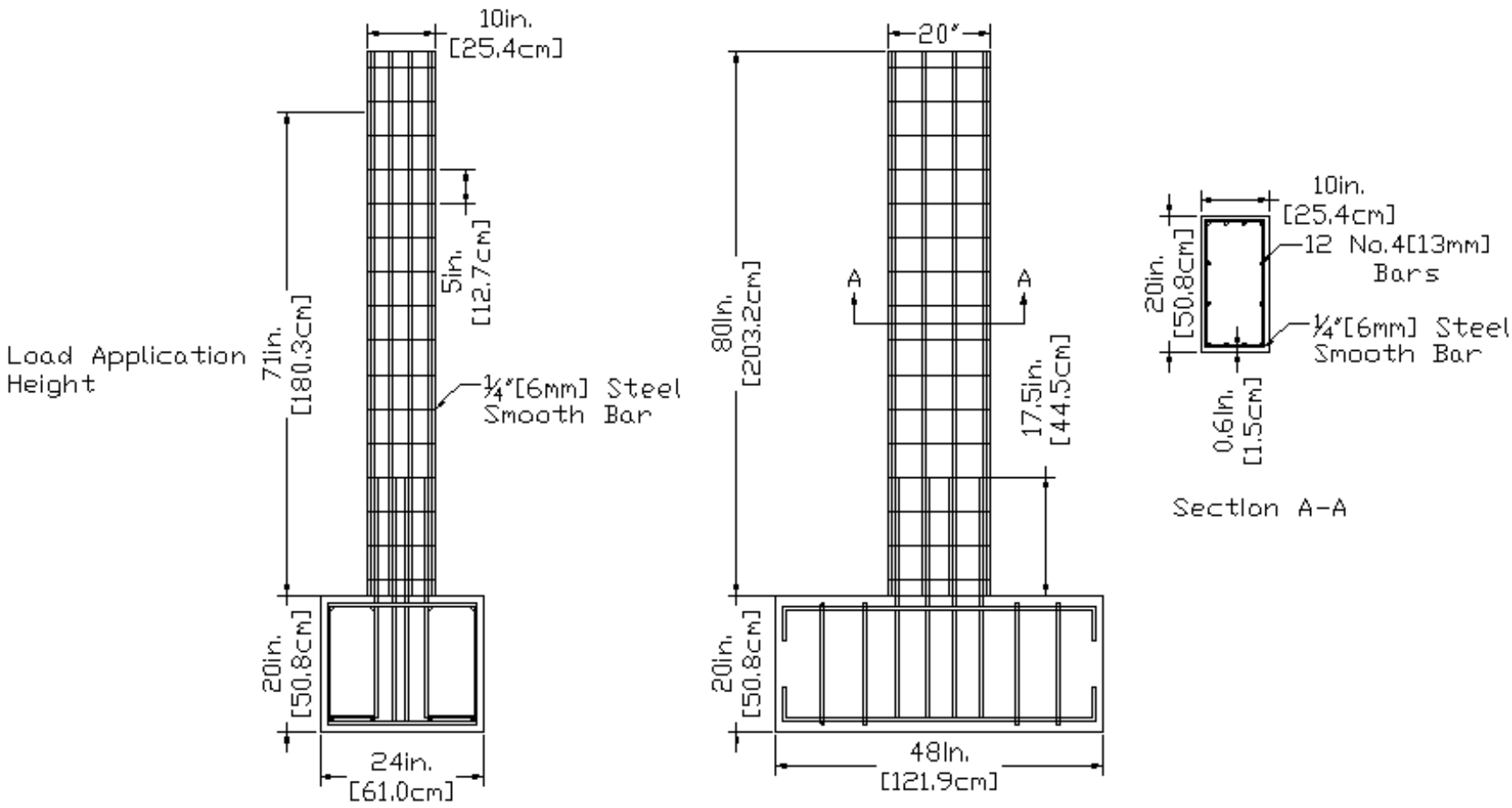

Figure 21 Details of Specimen AR-2

Specimens FRP-MS, FRP-4, FRP-6, FRP-8 and AR-2 were retrofitted using two plies (t_j = 0.1 in. (2.5 mm)), four plies (t_j = 0.2 in, (5.0 mm)), six plies (t_j = 0.3 in, (7.6 mm)), eight plies (t_j = 0.4 in, (10.2 mm)), and five plies (t_j = 0.25 in, (6.35 mm)) of CFRP, respectively. The CFRP covered the bottom 18 in. (46 cm) of Specimens FRP-MS, FRP-4, FRP-6 and AR-2. For Specimen FRP-8, half of the total CFRP covered the bottom 18 in. (46 cm) (4 plies), while the other half was applied only to the bottom 4 in. (10 cm) (8 plies) to investigate the effects of increased jacket thickness applied locally at the bottom of the jacket. A gap of 0.5 in. (12.5 mm) was provided between the CFRP jacket and the footing for columns retrofitted with rectangular CFRP jackets, while Specimen FRP-MS with the oval-shaped jacket had a 1.0 in. (12.5 mm) gap. A summary of the CFRP retrofitting measures is provided in Figure 22.

The rectangular cross-section of the Specimen FRP-MS was modified into an oval section before retrofitting. A steel jacket similar to the one used in Specimen SJ was temporarily positioned over the bottom 18 in. (46 cm) of the column. Instead of welding the vertical seams of the steel jacket, four bolts were installed to hold the steel jacket components together. After positioning the steel jacket around the specimen, the gap between the jacket and the column was filled with a high-strength non-shrink grout. Once the grout cured, the steel jacket was removed and the CFRP wrapping was installed around the oval-shaped grout section. The other specimens with CFRP retrofitting were provided with rectangular jackets.

A dry lay-up method in accordance with the manufacturer's recommendations was used to install the CFRP. To avoid stress concentrations on the CFRP, the corners of the rectangular columns were rounded to a 0.5 in. (12.5 mm) radius before the CFRP was

applied. The surface of the column to which the retrofitting was to be installed was then abraded to smooth out irregularities and to provide more surface area for adhesion. In order to promote bonding and prevent the surface from drawing resin away from the CFRP, a low viscosity epoxy primer was applied with a roller until the column surface was saturated. One more coat of epoxy was applied on the column, and the CFRP was then installed. Finally, another coat of epoxy was applied on top of the wrapped CFRP. This process was repeated until the desired number of layers was installed. Figure 23 summarizes the CFRP installation process.

Specimen FRP-MS

Specimen FRP-MS was retrofitted using an oval-shaped CFRP jacket. Figure 24 shows the lateral load vs. horizontal displacement hysteresis curves for Specimen FRP-MS. This specimen achieved a displacement ductility level of 7.2 while maintaining the axial load resisting capacity throughout testing. Failure in Specimen FRP-MS occurred while loading to the second cycle of the +3.2 in. (+81 mm) displacement level. The hysteresis response of Specimen FRP-MS is similar to that for Specimen SJ, except that Specimen FRP-MS resisted slightly higher lateral loads. The maximum lateral load resisted by Specimen FRP-MS was 16.1 kips (72 kN) and occurred at a lateral displacement of 2.4 in. (61 mm).

Most of the damage in Specimen FRP-MS occurred in the 1 in. (25.4 mm) gap provided between the added oval-shaped retrofit section and the footing. However, small horizontal flexural cracks also occurred up to the mid-height of the column. At a displacement level of 1.2 in. (30 mm), a flexural crack within the gap region became

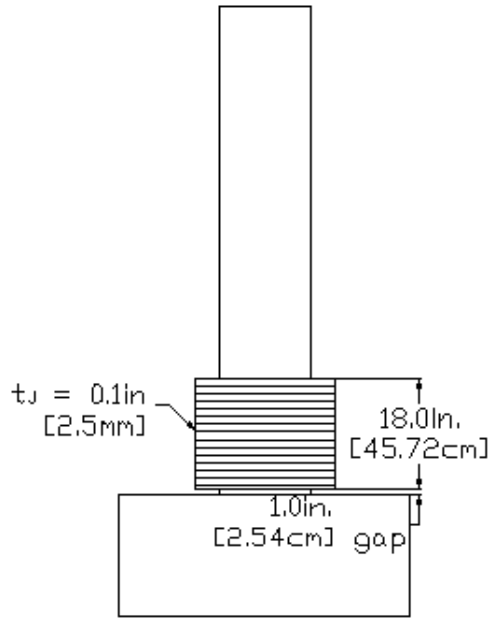

a) Specimen FRP-MS

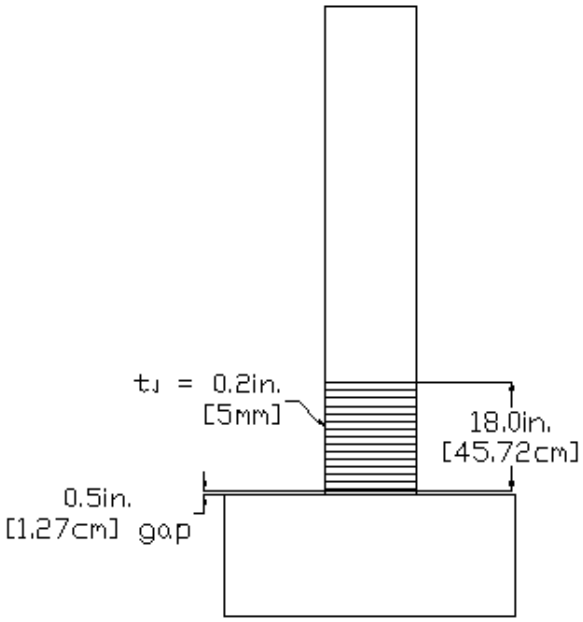

b) Specimen FRP-4

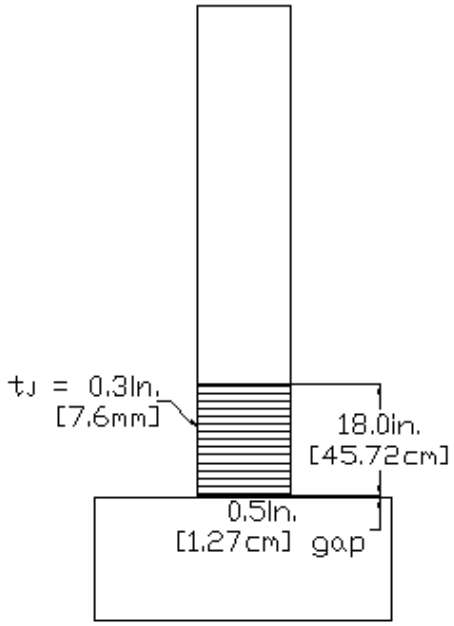

c) Specimen FRP-6

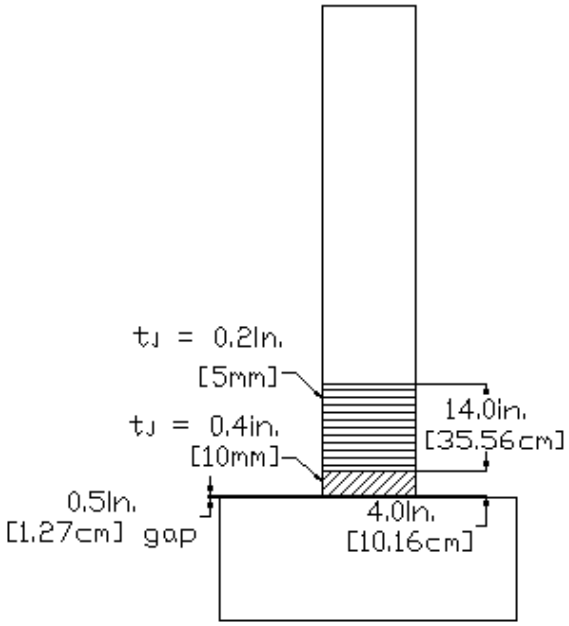

d) Specimen FRP-8

Figure 22 Summary of CFRP Jackets

a) Smooth Out Irregularities

b) Saturate Column Surface with Epoxy

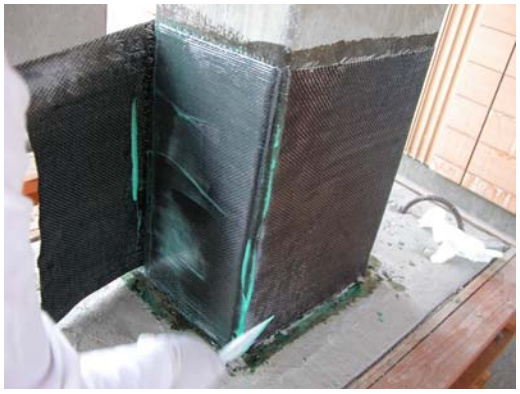

c) Install CFRP Wrapping

d) Saturate CFRP with Epoxy

Figure 23 Steps for CFRP Retrofit Installation

noticeable. The concrete in the gap region began to crush and spall, as shown in Figure 25, at a displacement level of 1.6 in. (30 mm) and exposed the column reinforcement. Buckling of the reinforcement was observed in the gap region during the first cycle at the 2.4 in. (61 mm) displacement level. A "popping" sound was heard during the second cycle at 3.2 in. (81 mm) due to a low-cycle fatigue fracture of a longitudinal bar. After the column's lateral load resisting capacity dropped below 80% of the peak load, four other longitudinal bars ruptured while loading to a displacement level of 4 in. (102 mm).

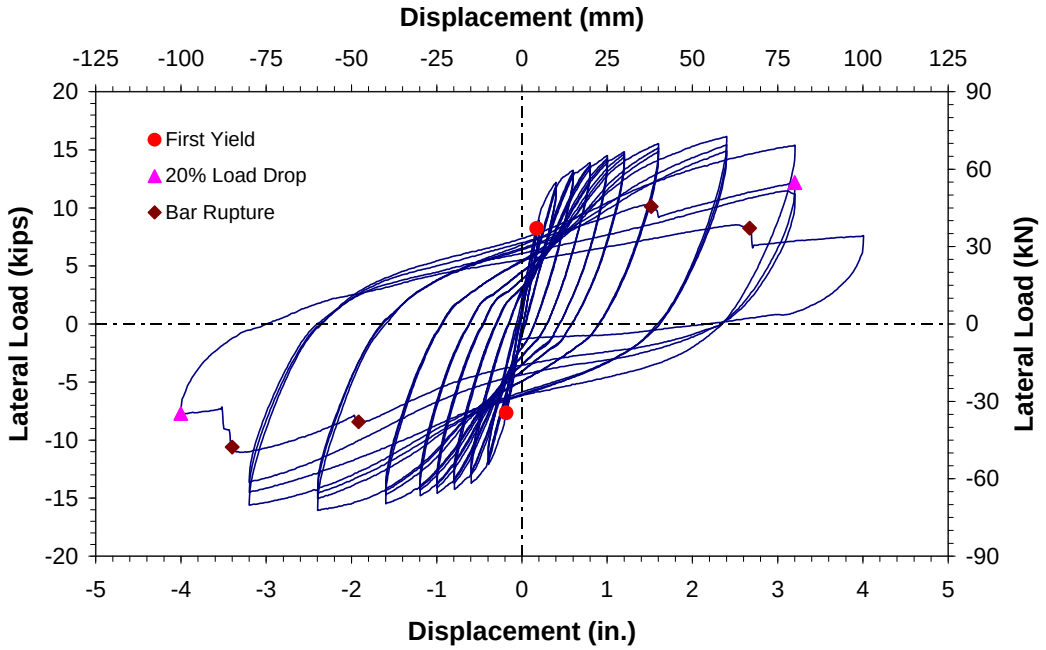

Figure 24 Lateral Load vs. Displacement Hysteresis Curves for Specimen FRP-MS

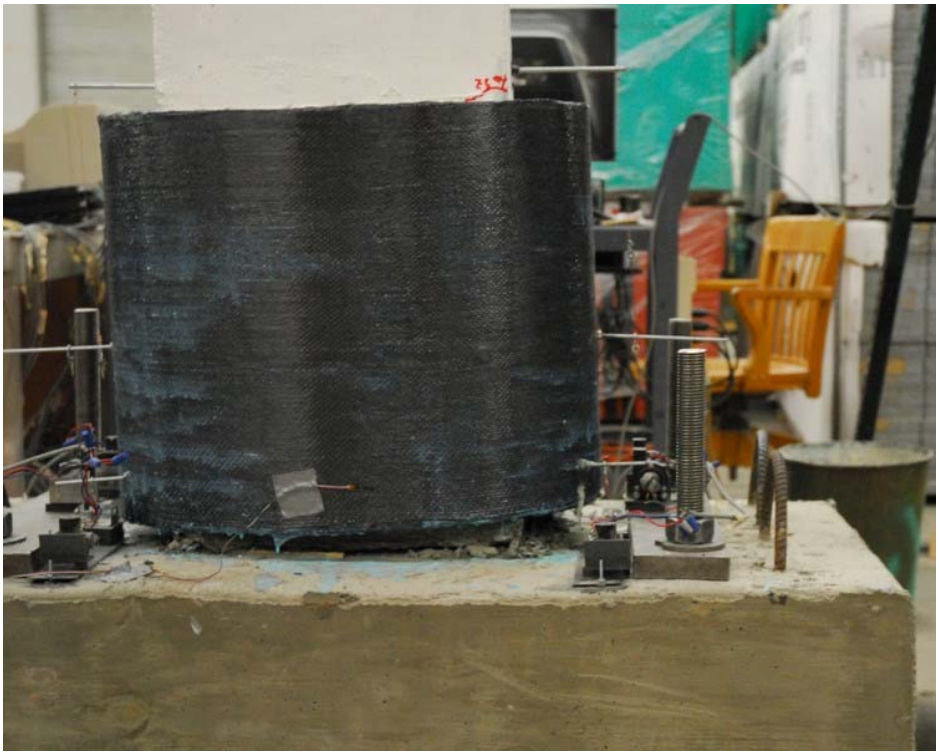

Figure 25 Specimen FRP-MS During Testing

Strain gages on the oval CFRP jacket recorded a maximum strain value of 140 microstrain. Even with this minimal strain in the CFRP, the jacket provided sufficient confinement to the column that prevented yielding in the bottom transverse hoop. The maximum tensile strain measured in the hoop was 380 microstrain, approximately 25% of the yield strain. The starter bars showed high levels of strain exceeding the strain gage capacity of 10,000 microstrain.

Specimen FRP-4

Specimen FRP-4 was retrofitted in accordance with the recommendations of ACTT-95/08 (Seible et al., 1995) and consisted of 4 layers of CFRP applied as a rectangular-shaped jacket. The hysteresis curves for Specimen FRP-4 are shown in Figure 26 and indicate good energy dissipation. Failure in this specimen occurred during the third cycle of the 3.2 in. (81 mm) displacement level, corresponding to displacement ductility level of 7.4. The specimen experienced a peak lateral load of 16.9 kips (75 kN) at a displacement of 2.4 in. (61 mm). The hysteresis response for Specimen FRP-4 is similar to that obtained for both specimens with oval-shaped jacketing.

At the end of testing, Specimen FRP-4 was still capable of sustaining the applied axial load, and there was no sign of rupture of the CFRP jacket. However, a significant bulging of the jacket, as shown in Figure 27, was observed on the flat sections of the CFRP retrofit. Within the 0.5 in. (12.5 mm) gap provided at the base of the column, a significant horizontal flexural crack developed during testing, as shown in Figure 28. Flexural cracking in the column section above the retrofit was also observed. The specimen experienced no significant drop in load until the longitudinal bars started to

fracture during the third cycle of the 3.2 in. (81 mm) displacement level due to low-cycle fatigue rupture.

The maximum strain recorded in the CFRP jacket was approximately 2000 microstrain. The rectangular jacket provided confinement that reduced tensile strains in the bottom transverse hoop when compared to the as-built specimens. The maximum tensile strain measured in the hoop was 1550 microstrain, approximately 85% of the yield strain. The starter bars showed high levels of strain exceeding the strain gage capacity of 10,000 microstrain.

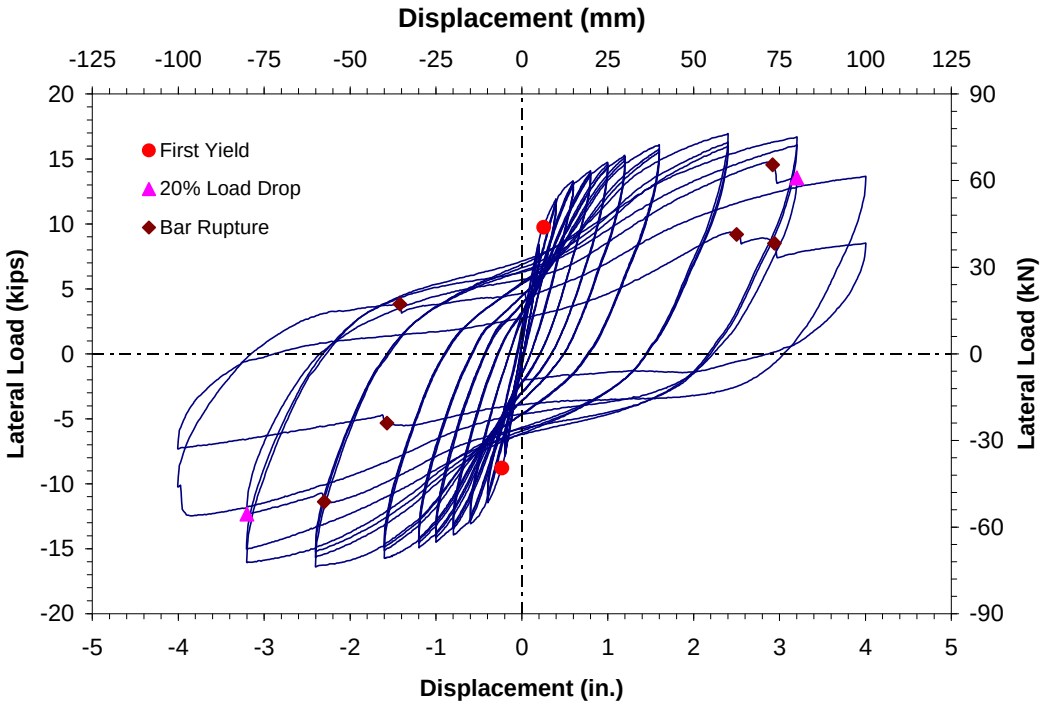

Figure 26 Lateral Load vs. Displacement Hysteresis Curves for Specimen FRP-4

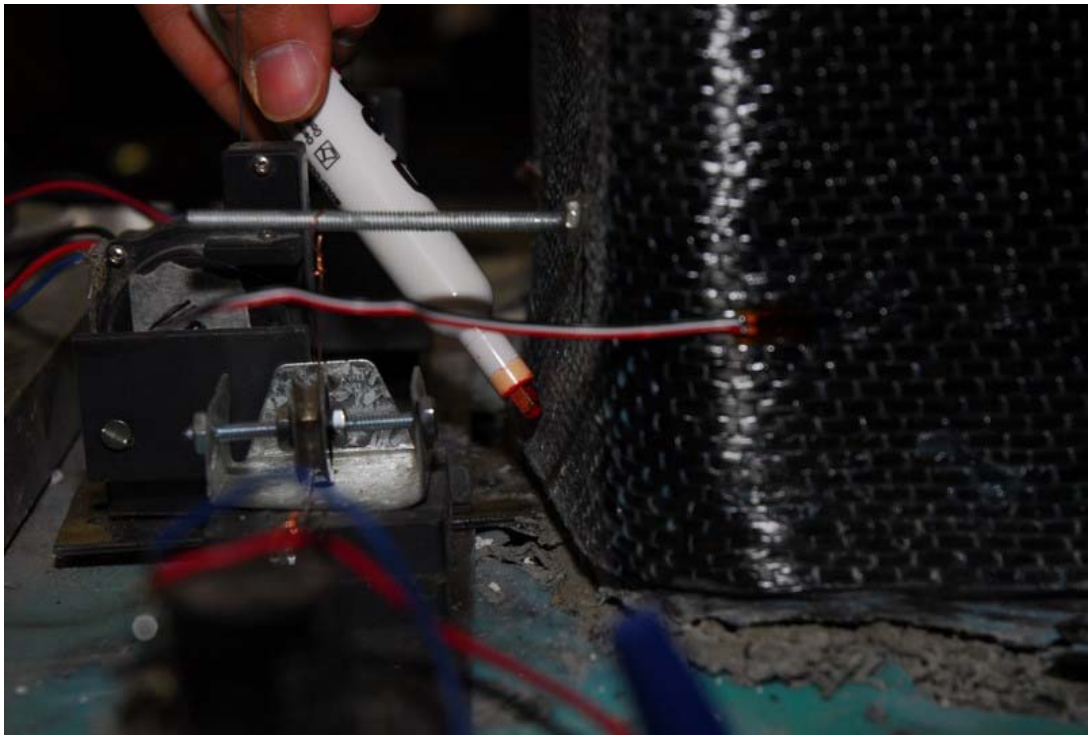

Figure 27 Bulging at the base of Specimen FRP-4

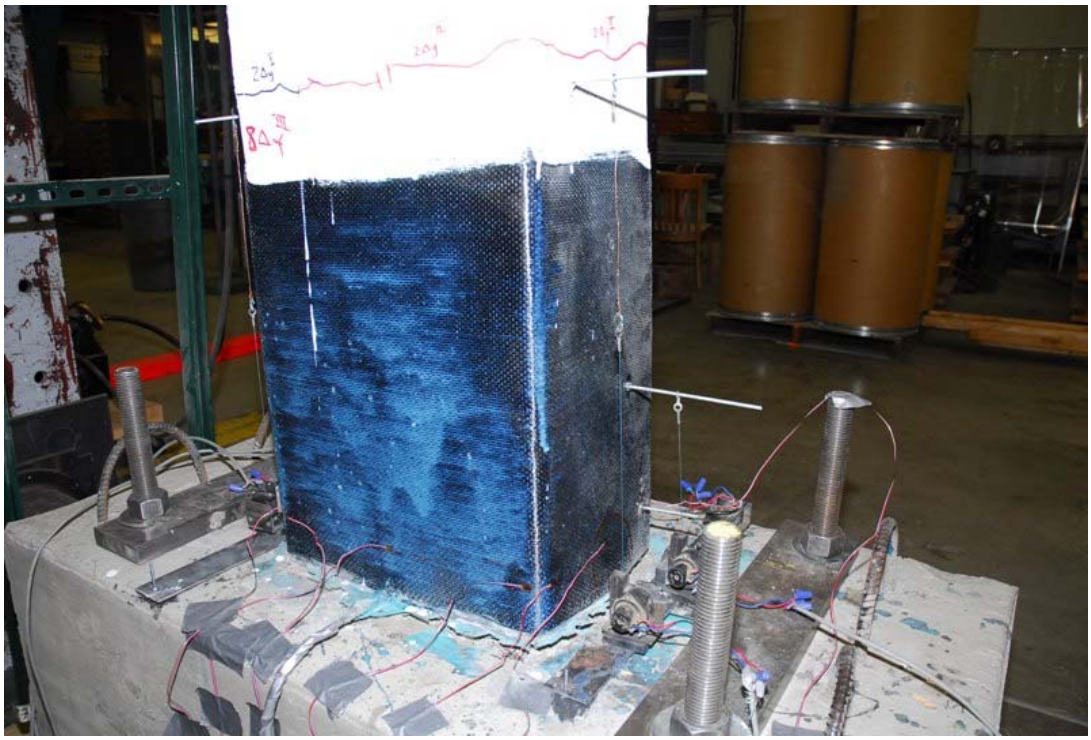

Figure 28 Specimen FRP-4 During Testing

Specimen FRP-6

Specimen FRP-6 was retrofitted based on 150% of the recommendations of ACTT-95/08 (Seible et al., 1995) and consisted of 6 layers of CFRP applied as a rectangular-shaped jacket. The lateral load vs. displacement hysteresis curves for Specimen FRP-6 are given in Figure 29. Specimen FRP-6 achieved a displacement level of 4 in. (102 mm), which corresponds to a displacement ductility of 9.1. At a displacement of 2.4 in. (61 mm), the column resisted a peak lateral load of 17.4 kips (77 kN). Failure in Specimen FRP-6 occurred on the second cycle of the 4 in. (102 mm) displacement level where a rapid loss of stiffness and load resisting capacity occurred due to the rupture of four longitudinal bars. Even at this stage, the column was able to carry the applied axial load.

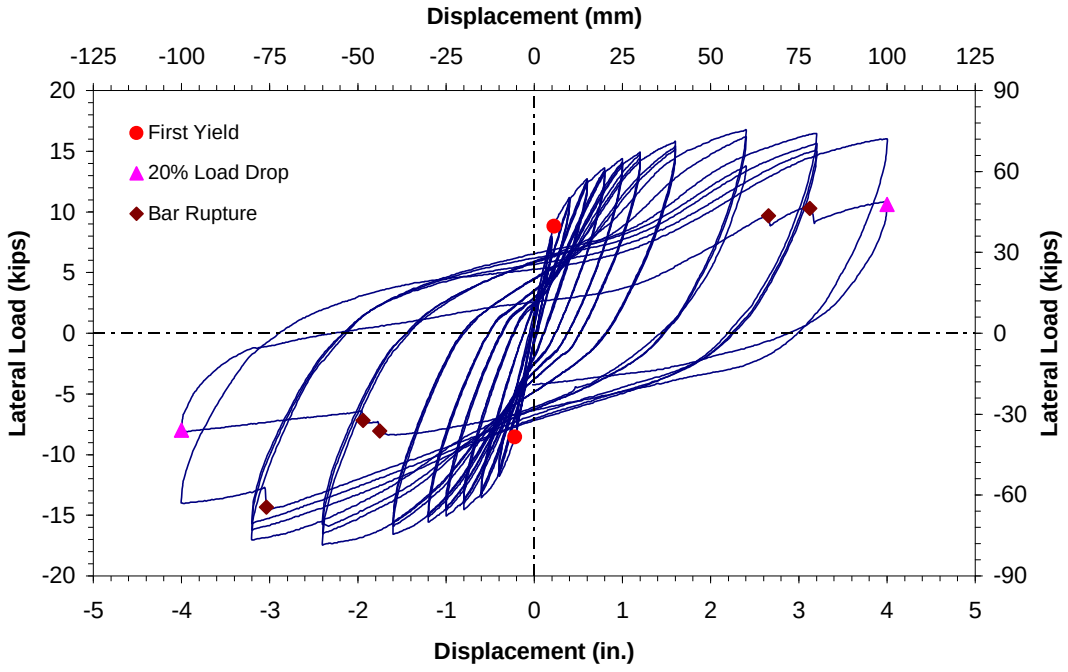

Figure 29 Lateral Load vs. Displacement Hysteresis Curves for Specimen FRP-6

The failure mechanism of Specimen FRP-6 was similar to that of Specimen FRP-4. A major flexural crack, shown in Figure 30, developed in the gap region between the column and the footing, and minor flexural cracks were noticed above the CFRP jacket, as shown in Figure 31. The CFRP jacket in Specimen FRP-6 experienced only minor bulging at the column base at the end of testing.

The performance of Specimen FRP-6 was superior to that of the as-built specimens and all other retrofitted specimens. The specimen was able to resist the applied load without a noticeable drop until the longitudinal bars started to fracture. The applied retrofit also delayed bar rupture until a lateral displacement of 4 in. (102 mm) was reached. The additional load cycles substantially enhanced energy dissipation in this specimen.

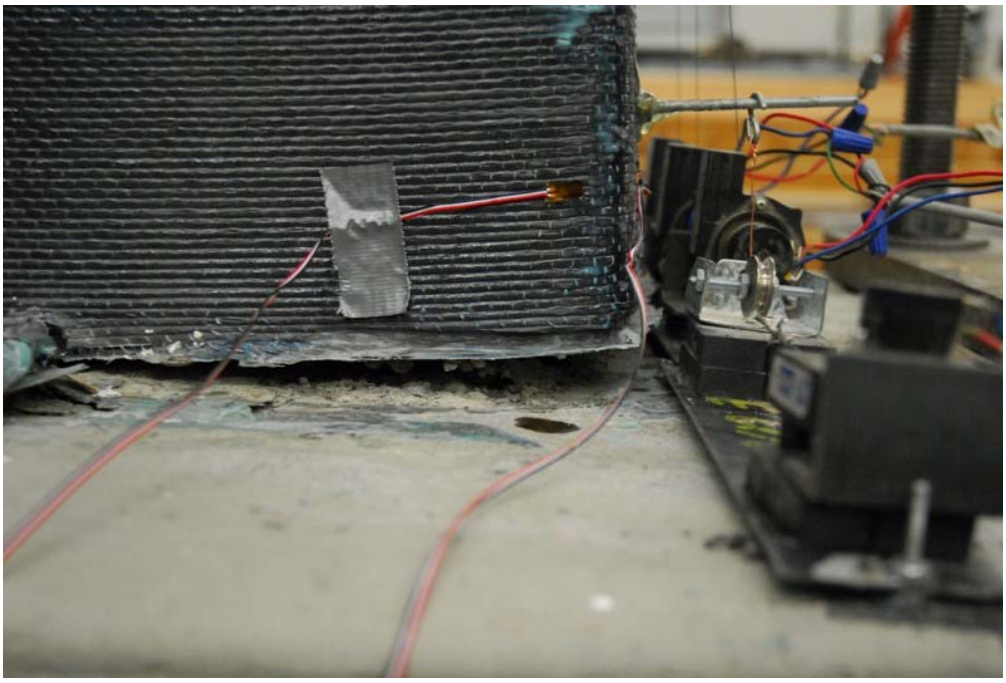

Figure 30 Flexural Crack at the Base of Specimen FRP-6

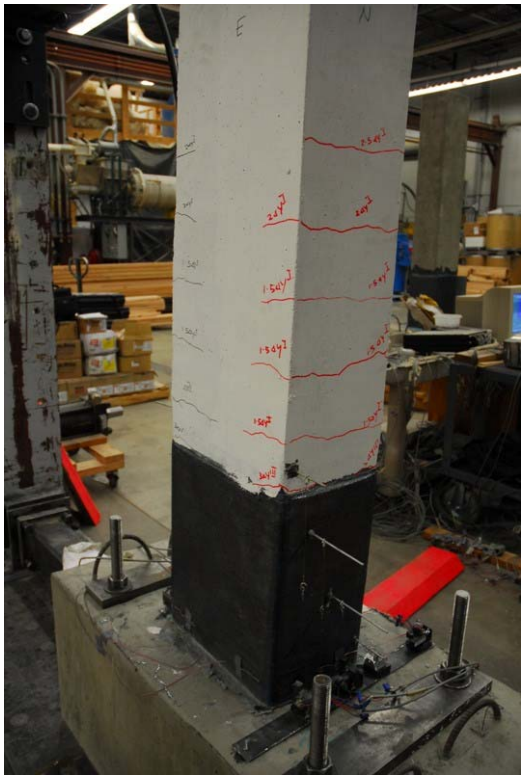

Figure 31 Specimen FRP-6 During Testing

Strain gages on the CFRP jacket recorded a maximum strain of approximately 1200 microstrain. The rectangular jacket provided external confinement that reduced the tensile strain level in the bottom transverse hoop compared to that in the as-built specimens. The maximum tensile strain measured in the hoop was 1480 microstrain, approximately 80% of the yield strain. The starter bars showed high levels of strain exceeding the strain gage capacity of 10,000 microstrain.

Specimen FRP-8

Specimen FRP-8 was retrofitted based on 200% of the recommendations of ACTT-95/08 (Seible et al., 1995) and consisted of 8 layers of CFRP applied as a rectangular-shaped jacket. Four CFRP layers were applied over the bottom 18 in. (46

cm), and the remaining 4 layers were applied only to the bottom 4 in. (10 cm). The lateral load vs. displacement hysteresis curves for Specimen FRP-8 are given in Figure 32. Failure in Specimen FRP-8 occurred during the second cycle of the 3.2 in. (81 mm) displacement level, corresponding to a displacement ductility of 7.3. The peak lateral load was 17.6 kips (78 kN) and occurred at a lateral displacement of 2.4 in. (61 mm). Similar to the other retrofitted columns, Specimen FRP-8 was able to sustain its lateral load capacity until the longitudinal bars began to rupture.

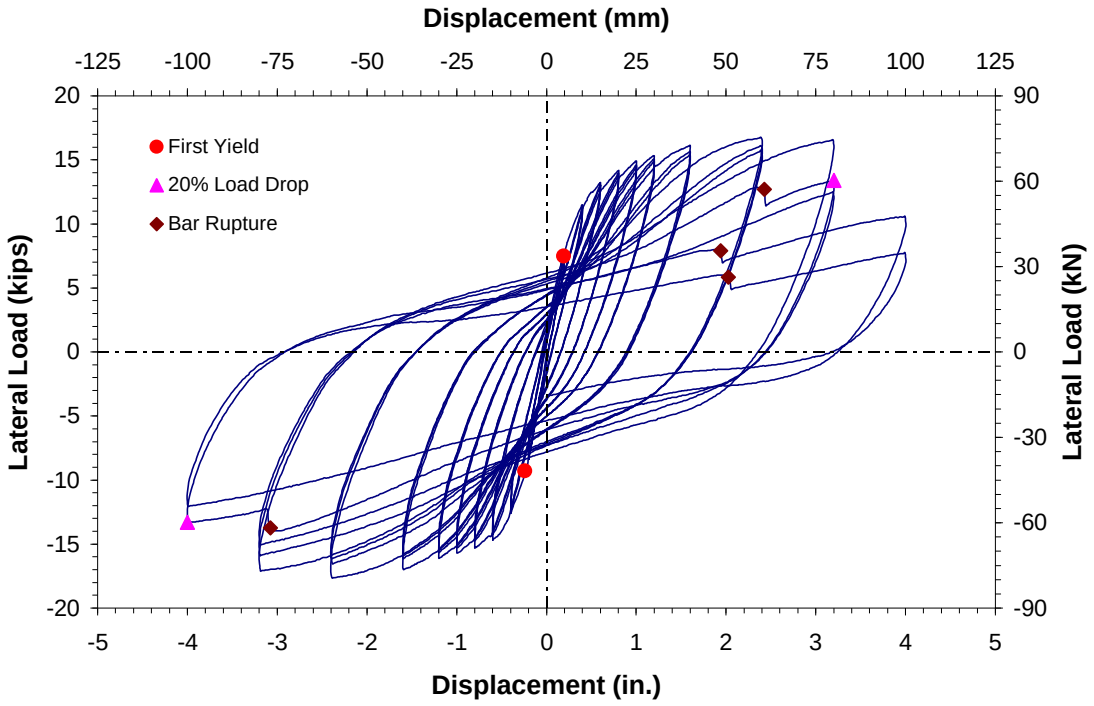

Figure 32 Lateral Load vs. Displacement Hysteresis Curves for Specimen FRP-8

Upon completion of testing, the CFRP jacket showed no sign of rupture, but minor bulging was noticed at the base of the column. The level of bulging in Specimen FRP-8 was comparable to that of Specimen FRP-6. Crack patterns observed in Specimen FRP-8 were essentially the same as for Specimen FRP-6. Figure 33 shows the small

flexural cracks that appeared above the jacket, and the major crack that developed within the gap region at the base of the column is shown in Figure 34. Specimen FRP-8 was expected to perform better than other columns retrofitted with rectangular jackets because of its thicker CFRP jacket. However, bar rupture limited the improvement in the displacement ductility.

The strain gages on the CFRP jacket recorded a maximum strain of 1470 microstrain. The rectangular CFRP jacket provided confinement that reduced the tensile strain level of the bottom transverse hoop compared to that for the as-built specimens. The maximum tensile strain measured in the bottom hoop was 800 microstrain, approximately 45% of the yield strain. The starter bars showed high levels of strain exceeding the strain gage capacity of 10,000 microstrain.

Figure 33 Specimen FRP-8 During Testing

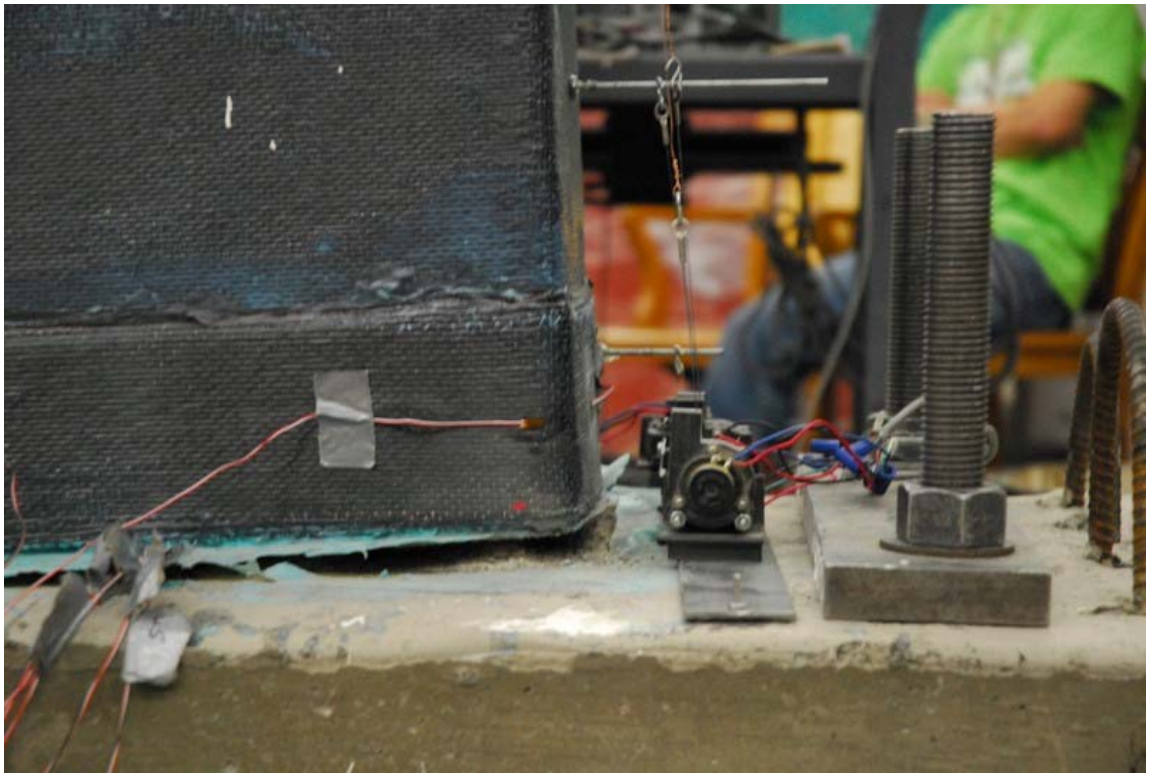

Figure 34 Flexural Crack at the Base of Specimen FRP-8

Specimen AR-2

Specimen AR-2 was the only specimen with a cross-sectional aspect ratio of 2. Although the ACTT-95/08 recommendations apply to rectangular columns with a cross-sectional aspect ratio of 1.5 or less, the CFRP wrapping on Specimen AR-2 was based on these recommendations in order to examine if the constraints on the cross-sectional aspect ratio contained in these guidelines could be expanded. Five layers of rectangular CFRP were applied on Specimen AR-2

Figure 35 shows the lateral load vs. horizontal displacement hysteresis curves for this specimen. This specimen was able to achieve a displacement ductility level of 7 while maintaining the axial load resisting capacity throughout testing. This specimen

failed on the third cycle at the 2.4 in. (61 mm) displacement level. The maximum lateral load resisted by Specimen AR-2 was 26.7 kips (119 kN) at a lateral displacement of 1.8 in. (46 mm). The lateral load resisting capacity did not start to degrade until the longitudinal bars began to rupture due to low-cycle fatigue.

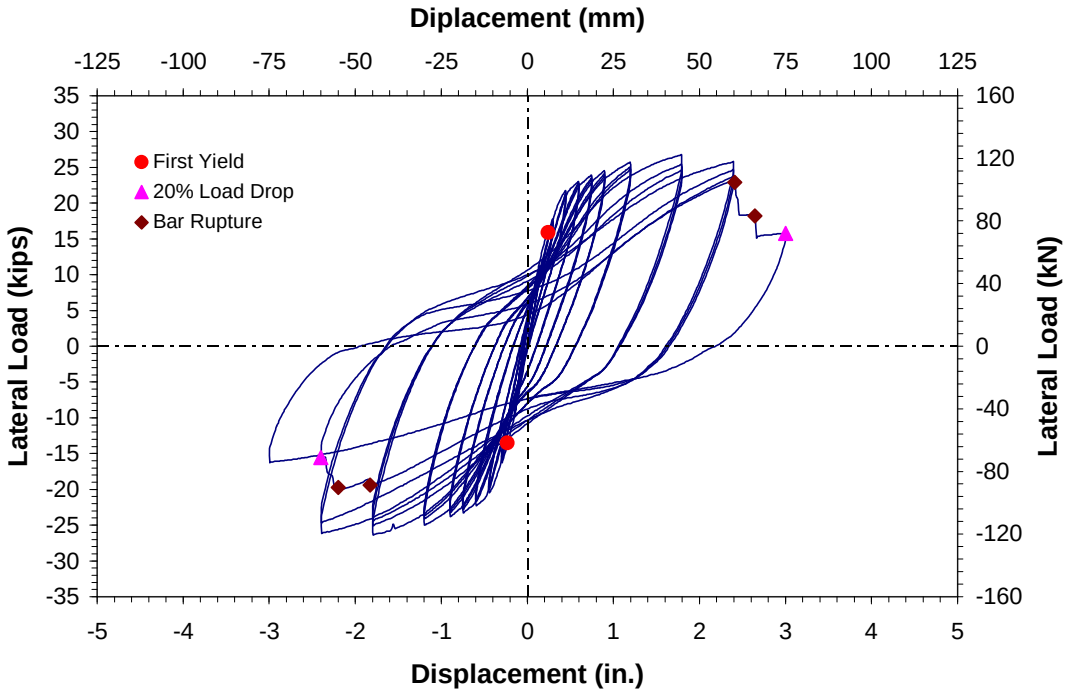

Figure 35 Lateral Load vs. Displacement Hysteresis Curves for Specimen AR-2

A photograph of Specimen AR-2 during testing is shown in Figure 36. The level of damage and the crack patterns for Specimen AR-2 were similar to the other specimens retrofitted with CFRP rectangular jackets. A significant flexural crack developed in the gap region at the base of column. Smaller flexural cracks developed in the column above the CFRP jacket. Bulging of the jacket, shown in Figure 37, occurred in the plastic hinge region toward the end of testing and was similar in extent to that for Specimen FRP-4. In general, the performance of Specimen AR-2 was similar to the retrofitted specimens with

cross-sectional aspect ratio of 1.5, but with a slightly lower displacement ductility capacity.

The strain gages on the CFRP wrapping recorded a maximum strain of 3500 microstrain. The rectangular jacket provided external confinement that reduced the strains in the bottom transverse hoop. The maximum tensile strain measured in the hoop was 1800 microstrain, approximately 95% of the yield strain. The starter bars showed high levels of strain exceeding the strain gage capacity of 10,000 microstrain.

Figure 36 Specimen AR-2 During Testing

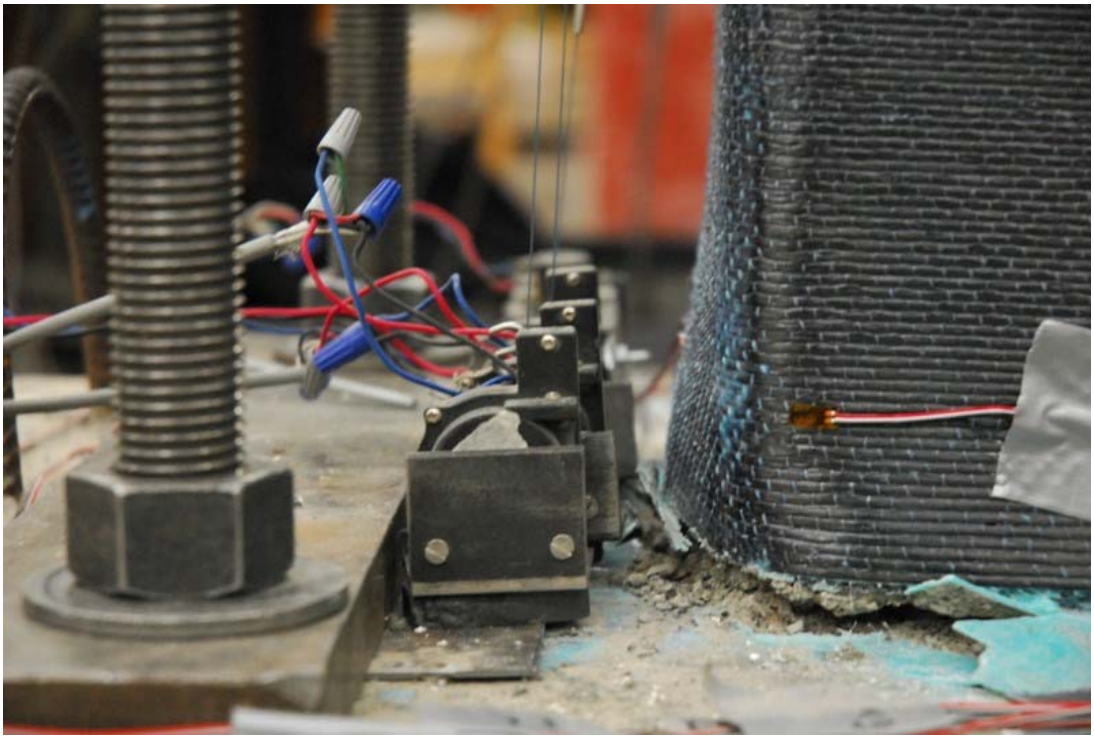

Figure 37 Bulging at the Base of Specimen AR-2

Summary of CFRP Jacketed Specimen Tests

Failure in all of the CFRP jacketed specimens was caused by the formation of a flexural hinge at the base of the column leading to eventual low-cycle fatigue fracture of the longitudinal reinforcement. No slippage of the lapped bars occurred during testing. The retrofitted columns achieved displacement ductilities of approximately 7, except for Specimen FRP-6 which attained a displacement ductility of 9.1. Specimen FRP-6 attained one more displacement level than the other columns before the longitudinal reinforcement began to fracture.

Strains occurring in the transverse hoop reinforcement are an indication of the core concrete dilation level. Therefore, the maximum strains in the hoops can be used to compare the level of confinement provided by the CFRP jackets. Specimen FPR-MS with

the oval shape provided the highest level of confinement and prevented yielding of the bottom transverse hoop. The rectangular CFRP jackets also did not allow yielding of the hoops, but higher levels of strains were measured in comparison to that for the oval-shaped retrofit. Of the specimens with rectangular CFRP jackets, Specimen FRP-8 had the highest level of confinement, followed by FRP-6, FRP-4 and AR-2 in decreasing order.

COMPARISON OF SPECIMEN PERFORMANCE

Backbone curves for the tested specimens were developed by connecting the measured loads at the end of each displacement level and are shown in Figure 38. Specimen AR2 is not included in the figure because of its different cross-sectional aspect ratio. As can be seen in Figure 38, the initial stiffness of all tested specimens was almost identical. This shows that the retrofit measures used in this study have little effect on column initial stiffness. In terms of strength, specimens with rectangular CFRP jackets created the upper bound on the backbone envelopes. The lower bound on the backbone curves was set by Specimen SJ, and may be due to some construction irregularities with that specimen. The as-built specimens resisted slightly lower peak lateral loads compared to those for the retrofitted specimens (except for Specimen SJ); the maximum difference in peak loads was 13%.

Table 2 lists the drift and displacement ductility achieved by each specimen. The as-built specimens achieved ductility levels of approximately 6, while the retrofitted specimens attained ductility levels of 7 or higher. Specimen FRP-6 attained the highest ductility level of approximately 9. The higher level of ductility in this specimen was a

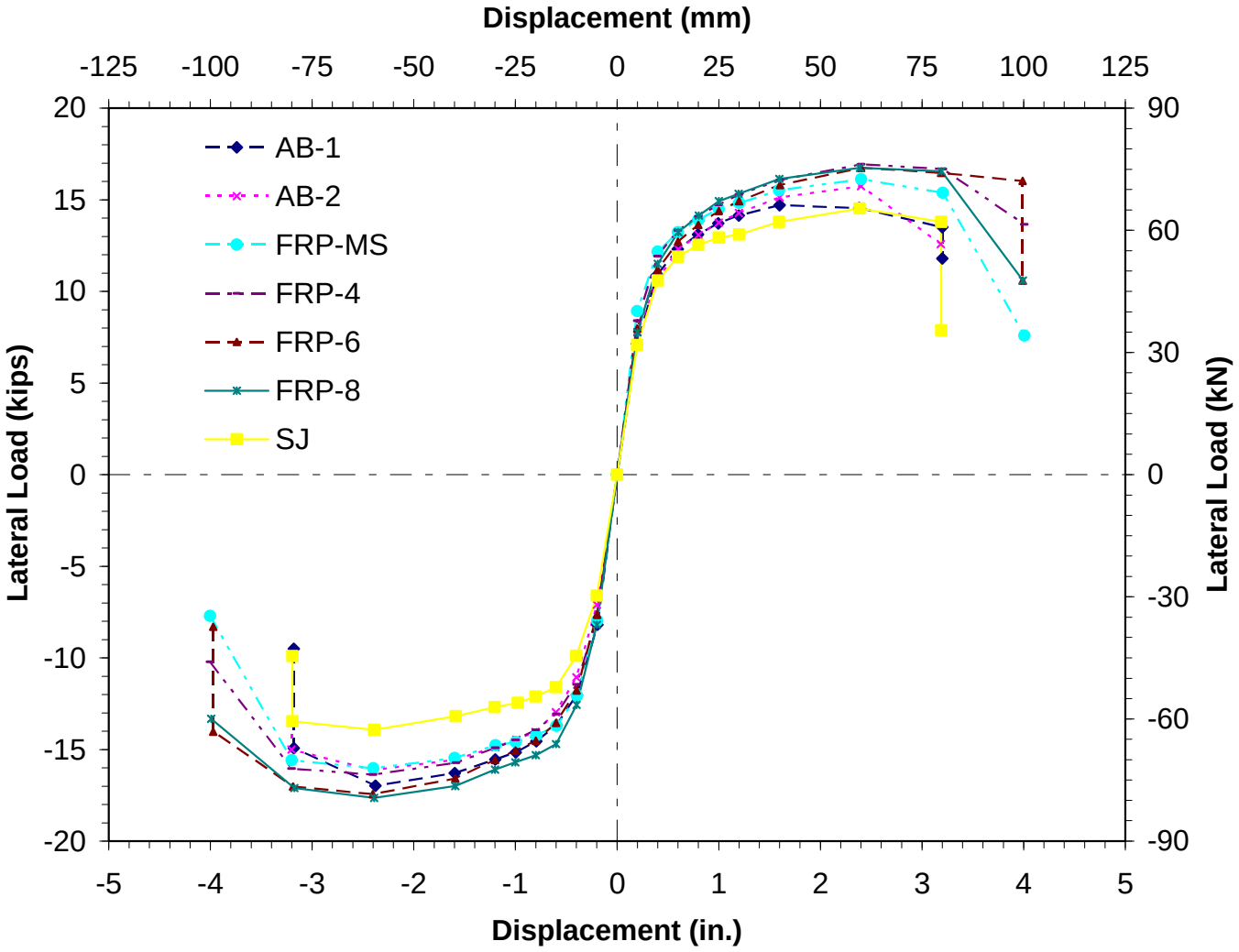

Figure 38 Backbone Curves for Tested Specimens

Table 2 Drift and Displacement Ductility of Tested Columns

Specimen	Effective Yield Displacement, in. (mm)	Measured Ultimate Displacement, in. (mm)	% Drift (Δ/L)	Displacement Ductility, μ_Δ
AB-1	0.50 (12.7)	3.2 (81)	4.5	6.4
AB-2	0.50 (12.7)	3.2 (81)	4.5	6.4
SJ	0.45 (11.4)	3.2 (81)	4.5	7.1
FRP-MS	0.47 (11.9)	3.4 (86)	4.8	7.2
FRP-4	0.50 (12.7)	3.7 (94)	5.2	7.4
FRP-6	0.44 (11.2)	4 (102)	5.6	9.1
FRP-8	0.48 (12.2)	3.5 (89)	4.9	7.3
AR-2	0.40 (10.2)	2.8 (71)	3.9	7

result of completing one more displacement cycle before the starter bars started to rupture due to a low-cycle fatigue.

Table 3 gives the maximum measured strain values in the bottom transverse hoop. The measured strains in the as-built specimens exceeded the strain gage capacity of 10,000 microstrain. The strain values listed in the table indicate that the oval CFRP and oval steel jacketing were the most effective retrofit methods for providing confinement. In comparison, there was a significant difference in the confinement provided by the oval and the rectangular CFRP retrofit jackets. However, the rectangular jackets did substantially reduce the hoop strains when compared to those in the as-built specimens. Table 3 shows that there was a direct relation between the amount of CFRP and the level of confinement for the rectangular CFRP jackets. Specimen FRP-8 had the lowest measured maximum strain, followed by FPR-6 and FRP-4. This implies that the

confinement level in Specimen FRP-8 was the highest followed by FRP-6 and FRP-4. The strain level in the bottom hoops also showed that the rectangular CFRP jacket was less effective in the column with higher cross-sectional aspect ratio (Specimen AR-2).

Table 3 Measured Peak Strains

Specimen	Max. Strain of Starter bars (microstrain)	Max. Strain of Bottom Hoops (microstrain)	Max. Strain of applied retrofit (microstrain)
AB-1	>10,000	>10,000	None
AB-2	>10,000	>10,000	None
SJ	>10,000	520	100
FRP-MS	>10,000	380	140
FRP-4	>10,000	1550	2000
FRP-6	>10,000	1480	1200
FRP-8	>10,000	800	1470
AR-2	>10,000	1800	3400

Energy dissipation can also be used to compare the performance of the tested specimens. The amount of energy dissipated per cycle is equal to the area within the lateral load vs. displacement hysteresis curve. For this study, the energy dissipated in the first cycle of all displacement levels before the lateral load resisting capacity dropped to 80% of the peak value was compared. Figure 39 shows the plot of cumulative dissipated energy vs. drift ratio (Δ/L). The plot indicates that there is no significant difference in the amount of energy dissipated per cycle. However, Specimen FRP-6 failed after

completing one more displacement level, and therefore it dissipated approximately 30% more energy when compared to that for the other specimens.

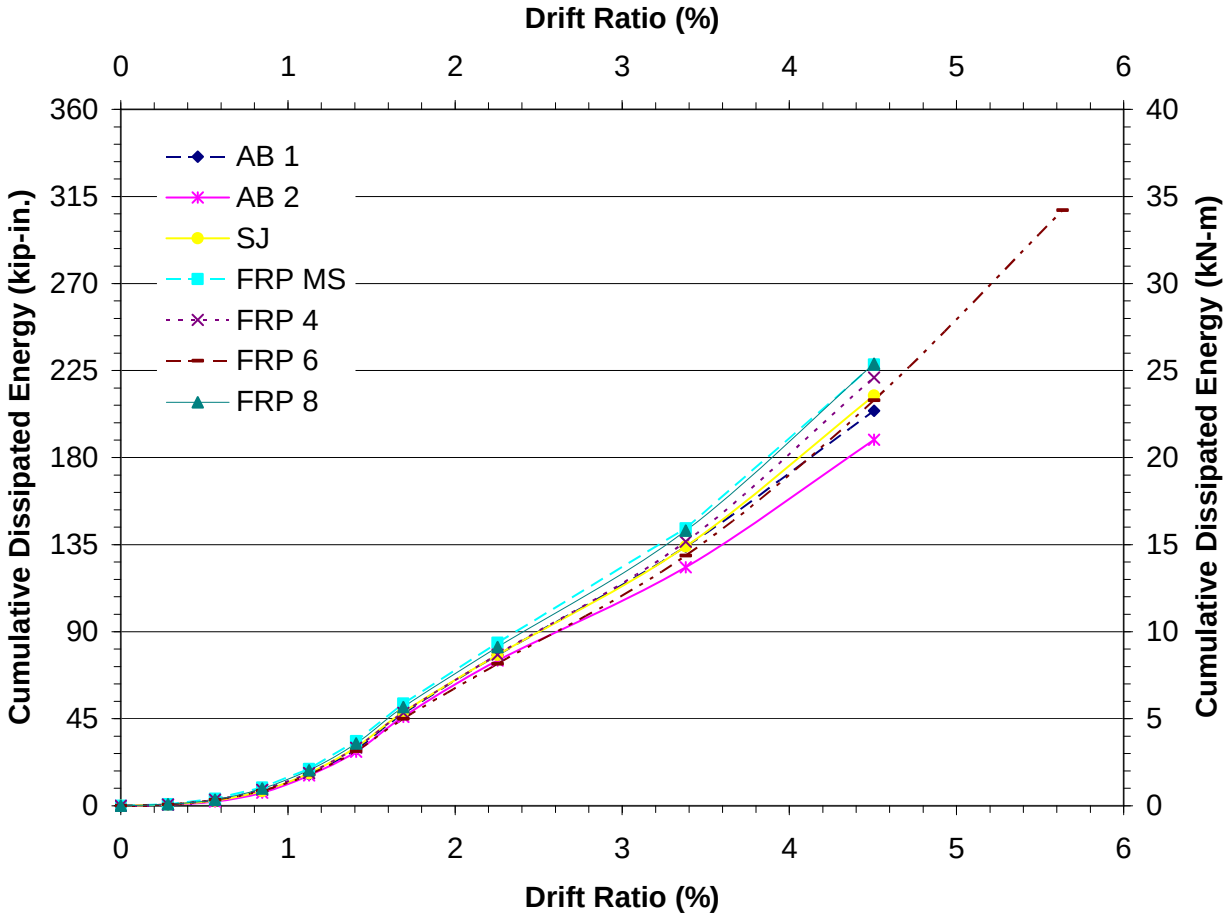

Figure 39 First Cycle Dissipated Energy vs. Drift Ratio

SUMMARY AND CONCLUSIONS

The experimental results of this study indicate that rectangular columns present in bridges in Washington State built in the 1950s and 1960s may perform better than has been reported for older bridge columns elsewhere in the U.S. Failure in the specimens representing the as-built conditions was caused by spalling due to flexural loading, leading to buckling and eventual low cycle fatigue fracture of the reinforcement along

with lap splice failure. Reasonable energy dissipation and ductility were achieved in the as-built specimens, reaching a displacement ductility level of 6. The superior performance obtained for the as-built specimens are due to specific parameters present in the columns of this study, namely a relatively long lap splice (35 times the spliced bar diameter), relatively low axial load (7% of the column axial capacity), and a low reinforcement content (1.2%). Although the investigated parameters are representative of columns in Washington State's interstate bridge inventory, caution is necessary in widely applying these conclusions to the performance of all existing rectangular bridge columns.

The column specimen retrofitted with an oval-shaped steel jacket demonstrated a ductile performance, reaching a displacement ductility level of 7. Failure in this specimen was due to flexural hinging in the gap region between the footing and retrofit jacket, leading to eventual low-cycle fatigue fracture of the longitudinal reinforcement. The column specimen retrofitted with an oval-shaped carbon fiber reinforced polymer (CFRP) jacket performed essentially the same as the steel-jacketed specimen, also achieving a displacement ductility of 7 and with the same failure mode.

Columns retrofitted with rectangular-shaped CFRP jackets all demonstrated ductile performance, achieving displacement ductilities of 7 or higher. Failure in these specimens was due to flexural hinging in the gap region followed by low-cycle fatigue fracture of the longitudinal reinforcement. No slippage of the lapped bars occurred during testing. The CFRP jacket designed based on ACTT-95/08 recommendations for rectangular-shaped retrofits resulted in performance similar to that for the specimens with oval-shaped jackets. Bulging of the CFRP jacket was observed towards the end of testing. Increased thickness of CFRP jackets resulted in reduced bulging of the CFRP jacket and,

in the case of the specimen retrofitted with a CFRP jacket designed based on 150% of the ACTT-95-08 recommendations, improved performance, achieving a displacement ductility of 9.

The retrofit measures of this study resulted in only modest improvements over the performance of the as-built specimens. This is due to the relatively good performance of as-built specimens that limited the available potential for improvement. Moreover, it should be noted that all retrofitted specimens achieved or exceeded a displacement ductility capacity of 7, which may be an acceptable performance level for all but the most severe seismic loading.

RECOMMENDATIONS

The results of this study provide a basis for evaluating and improving the seismic performance of existing rectangular bridge columns in Washington State. Analysis of an existing bridge must first be performed to identify the seismic demand on the columns. For low displacement ductility demands, columns with $35d_b$ lap splices at the base and with low axial load levels may not need retrofitting. While results from this study and from past research indicate satisfactory column performance for displacement ductility levels of 4 or more, it is conservatively recommended that all columns be retrofitted to ensure a ductile performance for displacement ductility demands of 2 or more.

For retrofitting of rectangular columns, it is recommended that oval-shaped jackets be used whenever possible. The oval jackets may be provided with steel or CFRP materials. Both types of jackets provide comparable levels of confinement that limit the transverse hoop strains to below 1000 microstrain and that produce ductile column

performance. Details and procedures for the design of oval-shaped steel jackets are provided in FHWA *Seismic Retrofitting Manual for Highway Bridges* (2006). Design guidelines for oval-shaped CFRP jackets are given in ACTT-95/08 (Seible et al., 1995). Oval-shaped jackets designed according to these recommendations can be expected to prevent slippage of lapped bars within the retrofitted region.

Rectangular-shaped CFRP jackets are also effective in improving the seismic performance of existing columns. While no slippage of the lap splice was observed in the retrofitted specimens of this study, it is conservatively recommended that rectangular-shaped CFRP wrapping be used only for the situation where controlled debonding of the lap splice is acceptable. A rectangular-shaped CFRP jacket with a thickness of 1.5 times the guidelines given in ACTT 95/08 is recommended for columns with cross section aspect ratio of 2 or less. The thickness of the CFRP jacket is determined based on the largest thickness required by considering three possible failure modes: flexural hinging, longitudinal bar buckling, and lap splice bond failure.

- The CFRP jacket thickness, t_j, required to provide for ductile flexural hinging at the base of a column is given by:

$$t_j = 3\left(0.09\frac{D_e(\varepsilon_{cu} - 0.004)f'_{cc}}{f_{ju}\varepsilon_{ju}}\right) \qquad \text{(Equation 19)}$$

  f_{ju} is the ultimate strength of the fiber, ε_{cu} is concrete's ultimate compression strain, D_e is the equivalent circular diameter and ε_{ju} is the strain of the fiber at failure. f'_{cc} is the compression strength of the confined concrete and can conservatively be taken as $1.5f'_c$ (Seible et al 1995).

- The CFRP jacket thickness needed to prevent buckling of the longitudinal bars in slender columns is given by:

$$t_j = \left(\frac{3nD_e}{E_j}\right) ksi \text{ or } t_j = \left(\frac{20.7nD_e}{E_j}\right) MPa \quad \text{(Equation 20)}$$

  n is the number of longitudinal bars and E_j is the modulus of elasticity of the jacket in ksi.

- The thickness required to prevent lap splice bond failure is given by.

$$t_j = 3\left(500\frac{D_e(f_l - f_h)}{E_j}\right) \quad \text{(Equation 21)}$$

  f_h is 0 for column with low transverse reinforcement ratios; D_e is an equivalent circular column diameter; and f_l is the lateral clamping pressure over the lap splice.

ACKNOWLEDGEMENTS

This research was conducted through the Washington State Transportation Research Center (TRAC) with funding from the Federal Highway Administration (FHWA) under contract DTFH61-03-C-00104. The technical contributions by Hamid Ghasemi of the FHWA and by DeWayne Wilson and Craig Boone of the Washington State Department of Transportation (WSDOT) Bridge Office are gratefully acknowledged.

REFERENCES

ACI 318-05 (2005). *Building Code Requirements for Structural Concrete and Commentary.* American Concrete Institute, Farmington Hills, Michigan.

ACI 440-02 (2002). *Guide for the Design and Construction of Externally Bonded FRP Systems for Strengthening Concrete Structures (ACI 440.2R-02).* American Concrete Institute, Farmington Hills, Michigan.

California Department of Transportation (1996). "Memo to Designers, 20-4"

Chai, Y. H.; Priestley, M. J. N.; Seible, F. (1991). "Retrofit of Bridge Columns for Enhanced Seismic Performance," *Seismic Assessment and Retrofit of Bridges, SSRP 91/03*, PP. 177-196.

Coffman, H. L.; Marsh, M. L.; Brown, C. B. (1993). "Seismic Durability of Retrofitted Reinforced-Concrete Columns," *ASCE Journal of Structural Engineering*, Vol. 119, No. 5, 1643-1661.

Endeshaw, Mesay A. (2008). "Retrofit of Rectangular Bridge Columns Using CFRP Wrapping," M.S. Thesis, Department of Civil and Environmental Engineering, Washington State University.

Ghosh, K. K. and Sheikh, S. A. (2007). "Seismic Upgrade with Carbon Fiber-Reinforced Polymer of Columns Containing Lap-Spliced Reinforcing Bars," *ACI Structural Journal*, Vol. 104., No. 2, 227-236.

Harajli, M. H. and Dagher, F. (2008). "Seismic Strengthening of Bond-Critical Regions in Rectangular Reinforced Concrete Columns Using Fiber-Reinforced Polymer Wraps," ACI Structural Journal, Vol. 105, No. 1, 68-77.

Haroun, M. A. and Elsanadedy, H. M. (2005). "Fiber-Reinforced Plastic Jackets for Ductility Enhancement of Reinforced Concrete Bridge Columns with Poor Lap Splice Detailing," *ASCE Journal of Bridge Engineering*, Vol. 1, No. 6, 749-757.

Harries, K. A.; Ricles, J. R.; Pessiki, S.; Sause, R. (2006). "Seismic retrofit of lap splices in nonductile square columns using carbon fiber-reinforced jackets," *ACI Structural Journal, Vol. 103*, No. 6, 874-884.

Iacobucci, R. D.; Sheikh, S. A.; Bayrak, O. (2003). "Retrofit of Square Concrete Columns with Carbon Fiber-Reinforced Polymer for Seismic Resistance," *ACI Structural Journal*, Vol. 100, No. 6, 785-794.

Lam, L. and Teng, J. G. (2003) "Design-Oriented Stress-Strain Model for FRP-Confined Concrete in Rectangular Columns," *SAGE Journal of Reinforced Plastics and Composites*, Vol. 22, No. 13 1149-1186.

Maalej, M.; Tanwongsval, S.; Paramasivam, P. (2003) "Modeling of Rectangular RC Columns Strengthened with FRP," *Elsevier Science Cement and Concrete Composites*, Vol. 25., No. 2, 236-276.

Memon, M. S. and Sheikh, S. A. (2005). "Seismic Resistance of Square Concrete Columns Retrofitted with Glass Fiber-Reinforced Polymer," *ACI Structural Journal*, Vol. 102, No. 5, 774-783.

Orangun, C. O., Jirsa, J. O., and Breen, J. E., (1977), "A Reevaluation of Test Data on Development Length and Splices," *ACI Journal Proceedings*, Vol. 74, No. 3, 114-122.

Priestley, M. J. N. and Seible, F. (1991). "Design of Seismic Retrofit Measures for Concrete Bridges," *Seismic Assessment and Retrofit of Bridges, SSRP 91/03*, University of California, San Diego, pp. 197-234.

Priestley, M. J. N., Seible, F. and Calvi, G. M. (1996). *Seismic Design and Retrofit of Bridges*, John Wiley & Sons, Inc., New York.

Seible, F.; Priestley, M. J. N.; Chai, Y. H. (1995). *Earthquake Retrofit of Bridge Columns with Continuous Carbon Fiber Jackets*, Advanced Composites Technology Transfer Consortium, Report No. ACTT-95/08, La Jolla, California.

Seismic Retrofitting Manual For Highway Structures: Part 1 - Bridges (2006). Federal Highway Administration, Report No. FHWA-HRT-06-032.

SEQAD Consulting Engineers (1993), *Seismic Retrofit of Bridge Columns Using High Strength Fiberglass/Epoxy Jackets*, Solana Beach, California.

Stapleton, S. E.; McDaniel, C. C.; Cofer, W. F.; McLean, D. I. (2005). "Performance of Lightly confined Reinforced Concrete Columns in Long-Duration Subduction Zone Earthquakes," *Transportation Research Record*, No. 1928, 185-192.

Washington State Department of Transportation (2006). "Bridge Design Manual M 23-50"

Xiao, Y. and Wu, H. (2003). "Compressive behavior of Concrete Confined by Various Types of FRP Composite Jackets," *SAGE Journal of Reinforced Plastics and Composites*, Vol. 22, No. 13, 1187-1202.